Interaction of the Human Prostacyclin Receptor and the NHERF4 Family member Intestinal and Kidney Enriched PDZ Protein (IKEPP)

Helen M. Reid, Elizebeth C. Turner, Eamon P. Mulvaney, Paula B. Hyland, Caitriona McLean and B. Therese Kinsella[†]
School of Biomolecular and Biomedical Sciences, Conway Institute of Biomolecular and Biomedical Research, University College Dublin, Belfield, Dublin 4, Ireland.

Corresponding author: Tel: 353-1-7166727; Fax: 353-1-7166456; Email: Therese.Kinsella@UCD.IE

Running Title: Interaction of IKEPP with the Prostacyclin Receptor.

Keywords: Prostacyclin Receptor, IKEPP, Interaction, Phosphorylation, NHERF, GPCR

Abbreviations
DDO, double drop-out; FTI, farnesyl transferase inhibitor; GPCR, G protein-coupled receptor; HA, hemagglutinin; hIP, human prostacyclin receptor; HUVEC, human umbilical vein endothelial cell; IKEPP, intestinal and kidney enriched PDZ protein; IP, prostacyclin receptor; NHERF, NA^+/H^+ exchange regulatory factor; PKA, cAMP-dependent protein kinase A; PL, phospholipase; PDZ, Postsynaptic density-95, Discs large, Zonula occludens-1; PDZK1, PDZ-domain-containing protein 1; QDO, quadruple drop-out; RBD, Rab11 binding domain; RLBA, radioligand binding assay; Y2H, yeast-two-hybrid.

Abstract
Prostacyclin and its I Prostanoid receptor, the IP, play central roles in haemostasis and in re-endothelialization in response to vascular injury. Herein, Intestinal and Kidney Enriched PDZ Protein (IKEPP) was identified as an interactant of the human (h) IP mediated through binding of PDZ domain 1 (PDZ^{D1}) and, to a lesser extent, PDZ^{D2} of IKEPP to a carboxyl-terminal Class I 'PDZ ligand' within the hIP. While the interaction is constitutive, agonist-activation of the hIP leads to cAMP-dependent protein kinase (PK) A and PKC- phosphorylation of IKEPP, coinciding with its increased interaction with the hIP. Ectopic expression of IKEPP increases functional expression of the hIP, enhancing its ligand binding and agonist-induced cAMP generation. Originally thought to be restricted to renal and gastrointestinal tissues, herein, IKEPP was also found to be expressed in vascular endothelial cells where it co-localizes and complexes with the hIP. Furthermore, *si*RNA-disruption of IKEPP expression impaired hIP-induced endothelial cell migration and *in vitro* angiogenesis, revealing the functional importance of the IKEPP:IP interaction within the vascular endothelium. Identification of IKEPP as a functional interactant of the IP reveals novel mechanistic insights into the role of these proteins within the vasculature and, potentially, in other systems where they are co-expressed.

1. INTRODUCTION

Post-synaptic density-95, discs-large, zonula occludens-1 (PDZ) domains are amongst the most frequently occurring protein:protein interacting domains, and act as molecular adaptors or scaffolds to modulate the expression and function of a vast array of proteins in species ranging from bacteria to man [1-3]. PDZ domains are small, modular entities that recognize 'PDZ ligands' located typically, but not exclusively, at the extreme C-termini of target proteins [1-3]. The canonical PDZ domain contains six β-sheets (βA – βF), a short α-helix (αA), and a long α-helix (αB) with a highly conserved 'GLGF' motif within its hydrophobic binding pocket, the so-called carboxylate binding loop (CBL), that is essential for the sequence specific recognition of the PDZ ligand within the target protein(s) [1-3]. The PDZ ligand itself may be grouped into one of three classes according to the residues at their *C-termini*; namely into Class I (Ser/Thr-X-Φ-COOH), II (Φ-X-Φ-COOH) and III (Asp/Glu-X-Φ-COOH), where Φ represents a hydrophobic amino acid and X can be any residue [1-3].

The Na^+/H^+ exchange regulatory factor (NHERF) family of PDZ-containing proteins comprises of 4 members including NHERF1(EBP50), NHERF2 (E3KARP), NHERF3 (PDZ domain-containing protein 1/PDZK1) and NHERF4 (intestinal and kidney enriched PDZ protein/IKEPP/PDZK2), where NHERF1/EBP50 and NHERF2 are the most widely distributed [4, 5]. Whereas NHERF1/EBP50 and NHERF2 contain only two PDZ domains each, the highly homologous PDZK1 and IKEPP each contain four PDZ domains [6, 7]. IKEPP was first identified in the kidney and gastrointestinal (GI) tract and, thus far, its expression has only been reported in these tissues [7-9]. In terms of its PDZ domain structure, IKEPP is the most divergent of the NHERF family [5]. Compared to the other NHERF family members, IKEPP has few known binding partners but amongst them include guanylyl cyclase C [7] and MAP17 [10]. IKEPP can also bind to NHE itself [11] and to a range of transporters including the type IIa Na-Pi co-transporter [8], the multidrug resistance protein 2 [12], the organic cation transport (OCT) family members OCT3, OCTN1 & OCTN2 [13], to the wild-type Cl/HCO_3 exchanger down-regulated in adenoma (DRA) [14] and to the cystic fibrosis transmembrane conductance regulator (CFTR) [15]. In all cases, the interactions are dependent on PDZ domain(s) within IKEPP itself and the individual/protein-specific PDZ ligands.

Prostacyclin, or prostaglandin (PG) I_2, is a member of the prostanoid family of arachidonic acid-derived autocoids that plays a central role in vascular haemostasis [16, 17]. It is an endothelium-derived vasodilator and inhibitor of platelet aggregation that also exerts potent pro-inflammatory and *anti*-proliferative effects [18-21]. In addition, prostacyclin promotes angiogenesis and re-endothelialization/vascular repair, thereby preventing restenosis in response to vessel injury [22, 23]. Imbalances in the levels of prostacyclin, or of its specific synthase or its receptor, are implicated in a range of vascular disorders including thrombosis, stroke, myocardial infarction, atherosclerosis, systemic and pulmonary hypertension [18, 19, 22]. In addition to its role in the vasculature, prostacyclin is centrally involved in other systems including in the kidney, where it regulates renal blood flow and glomerular filtration rate [24, 25], and in the lung where it acts as a bronchodilator and is widely implicated in the prevention of pulmonary arterial hypertension [26, 27].

The actions of prostacyclin are mainly mediated through 'the I prostanoid receptor' or, in short, 'the IP' [17], a member of the G protein-coupled receptor (GPCR) super-family. The IP is primarily coupled to Gs/adenylyl cyclase activation, but may also regulate other secondary effectors in a cell and/or tissue specific- manner [28-30]. The human (h)IP is somewhat unusual among GPCRs in that it undergoes both farnesylation, within an evolutionarily conserved 'Caa*X*' motif located at its extreme C-terminus [30, 31], and palmitoylation at Cys^{308}, Cys^{309} and Cys^{311} within its intracellular carboxyl-terminal (C)-tail domain, proximal to transmembrane domain (TM) 7 [32, 33]. While neither lipid modification affect the ligand binding properties of the hIP, they modulate its G protein coupling/intracellular signalling and, in the case of palmitoylation, may influence the ability of the hIP to directly interact with components of the intracellular trafficking machinery, including with Rab11a, to regulate agonist-induced intracellular trafficking of the hIP in response to receptor activation [31-34].

In addition to their classic interaction with heterotrimeric G-proteins, it is now recognized that GPCRs can interact with a wide range of functionally diverse proteins known collectively as 'GPCR interacting proteins' or 'GIPs', thereby regulating an array of other cellular events [35, 36]. Furthermore, mainly due to its divergent sequence and capacity to contain functionally distinct binding motifs, the intracellular C-tail domain of the GPCR is the critical binding domain for such interactions between GPCRs with their specific GIP(s) [35-37]. For example, the interaction of the hIP with its GIP, the GTPase Rab11a,

is dependent on a Rab11-binding domain (RBP) located within the proximal C-tail domain of the hIP, the orientation and interaction of the RBD with Rab11a may be dynamically regulated by agonist-dependent palmitoylation of the hIP at $Cys^{309} > Cys^{308}$ [33]. Furthermore, we have recently discovered that the hIP also interacts with the multi-PDZ domain protein PDZK1/NHERF3, through an interaction dependent on a Class I PDZ ligand located at its distal/extreme C-terminus [38]. Herein, we report the discovery of a novel, highly specific GIP interaction between the hIP and IKEPP, the NHERF4 family member. Hence, the overall aim of this study was to characterize this interaction and to determine the influence of IKEPP on hIP function. Data presented herein identify a novel agonist-regulated interaction between IKEPP and the hIP that is structurally and functionally distinct from the interaction previously identified between the closely related PDZK1/NHERF3 [38]. Moreover, we provide evidence that expression of IKEPP is not restricted to renal or gastrointestinal tissue but that it is also expressed in vascular endothelial cells, where it was found to play a key role in prostacyclin-induced endothelial cell migration and *in vitro* angiogenesis. The discovery that IKEPP is expressed in vascular endothelial cells where it interacts with the hIP to modulate endothelial cell migration and angiogenesis reveals a previously unknown role of IKEPP within the vasculature as well as suggesting new insights into the role of the hIP and IKEPP in other tissues, such as in the kidney, where both proteins are co-expressed.

2. MATERIALS AND METHODS

2.1. Materials Cicaprost was obtained from Schering AG (Berlin, Germany). RO1138452 was obtained from Cayman Chemicals; H-89 and Gö6983 were from Merck Biochemicals. Rabbit *anti*-IKEPP antibody was from Abcam®; mouse monoclonal *anti*-haemaglutinin (HA) 101R antibody was from Cambridge Biosciences; goat *anti*-IKEPP, normal rabbit IgG, horseradish peroxidase (HRP)-conjugated goat *anti*-rabbit, rabbit *anti*-goat and goat *anti*-mouse secondary antibodies were from Santa Cruz; rat monoclonal *anti*-HA 3F10-HRP-conjugated antibody was from Roche; rabbit *anti*-PhosphoSer antibody was from Invitrogen (61-8100); recombinant human vascular endothelial growth factor (VEGF) 165 (293-VE/CF) was from R&D Systems; mouse monoclonal *anti*-FLAG and *anti*-FLAG-HRP-conjugated M2 antibody, protein G-sepharose and protein A-sepharose were from Sigma-Aldrich; *anti*-HDJ-2 (DNAJ protein) was from Neomarkers; AlexaFluor488 goat *anti*-rabbit, and AlexaFluor594 goat *anti*-mouse antibodies were from Molecular Probes. Plasmids pCRE-Luc, pRL-TK and pCMVTag2C were from Agilent Technologies. Farnesyl transferase inhibitors R115777 and SCH66336 were obtained from Janssen Pharmaceuticals and Schering Plough, respectively. [^{3}H]iloprost was obtained from Perkin Elmer. All oligonucleotides were synthesized by Sigma Genosys.

2.2. Subcloning and site-directed mutagenesis

The plasmids pHM6:hIP^{WT}, pHM6:hIP^{SSLC} and pHM6:hIP$^{\Delta 383}$, encoding HA epitope-tagged forms of the wild type human prostacyclin receptor (hIP), isoprenylation defective hIP^{SSLC}, or Caa*X*-truncated hIP$^{\Delta 383}$, respectively, have been previously described [31]. The plasmid pHM6:hFP was generated by subcloning the full length sequence for the human $PGF_{2\alpha}$ (F) prostanoid receptor from pcDNA/Amp:hFP [39] into the *Kpn*I-*Eco*RI sites of the mammalian expression vector pHM6, such that its coding sequence was in-frame with the HA epitope-tag. The plasmid pcDNA3.1zeo:EP$_{3.1}$, encoding the HA-tagged EP$_3$ isoform of the PGE_2 receptor, was a gift from Dr Barrie Ashby [40]. The plasmids pGBKT7:hIP$^{299\text{-}386}$, pGBKT7:hIP$^{299\text{-}386,SSLC}$, pGBKT7:hIP$^{320\text{-}386}$, pGBKT7:hIP$^{299\text{-}320}$, pGBKT7:hIP$^{299\text{-}386,CSLS}$, pGBKT7:hIP$^{299\text{-}386,CSAC}$, pGBKT7:hIP$^{299\text{-}386,CSSC}$, pGBKT7:hIP$^{299\text{-}386,CALC}$, pGBKT7:hIP$^{299\text{-}383,C\text{-}STOP}$, pGBKT7:hIP$^{299\text{-}383,S\text{-}STOP}$, pGBKT7:hIP$^{299\text{-}386,CAAA}$, and pGBKT7:hIP$^{299\text{-}386,SAAA}$ were previously described [34, 38, 41]. The plasmids pACT2:IKEPP$^{1\text{-}287\ PDZD1*}$ and pACT2:IKEPP$^{1\text{-}287\ \ PDZD2*}$ were generated by QuikChange™ site-directed mutagenesis (Agilent Technologies) using the IKEPP library clone identified in the Y2H screen, pACT2:IKEPP$^{1\text{-}287}$, as template and the primer pairs shown in **Supplemental Table 1**. The plasmid pcDNA3:IKEPP was a gift from Dr Sharon Milgram, Bethesda, MD and the plasmids pCMVTag2C:IKEPP and pACT2:IKEPP were generated by subcloning the full-length sequence from pcDNA3:IKEPP into the *Eco*RI-*Xho*I sites of the mammalian expression vector pCMVTag2C or the yeast expression vector pACT2, such that its coding sequence was in-frame for FLAG epitope-tagged or HA epitope-tagged protein expression. The plasmids pACT:IKEPP^{PDZD1}, pACT:IKEPP^{PDZD2}, pACT:IKEPP^{PDZD3}, pACT:IKEPP^{PDZD4}, pACT:IKEPP$^{PDZD1\text{-}2}$, pCMVTag2C:IKEPP^{PDZD1}, pCMVTag2C:IKEPP^{PDZD2}, pCMVTag2C:IKEPP^{PDZD3}, pCMVTag2C:IKEPP^{PDZD4} & pCMVTag2C:IKEPP$^{PDZD1\text{-}2}$, encoding the individual PDZ domains, were generated by subcloning the sequences corresponding residues 1- 165 (PDZ^{D1}), 121 – 255 (PDZ^{D2}), 228 – 400 (PDZ^{D3}), 347 – 505 (PDZ^{D4}) and 1 - 255 (PDZ$^{D1\text{-}2}$) of IKEPP from pcDNA3:IKEPP into the *Eco*RI-*Xho*I sites of the yeast expression vector pACT2 or the mammalian expression vector pCMVTag2C. The plasmids pCMVTag2C:IKEPP^{PDZD1*}, pCMVTag2C:IKEPP^{PDZD2*}, pCMVTag2C:IKEPP^{PDZD3*}, pCMVTag2C:IKEPP^{PDZD4*}, pACT2:IKEPP^{PDZD1*}, pACT2:IKEPP^{PDZD2*}, pACT2:IKEPP^{PDZD3*}, and pACT2:IKEPP^{PDZD4*} where the respective hydrophobic binding pocket ("*GLGF*") sequence for each PDZ domain [42] was mutated from SF^{60}G^{61}F to S$\underline{R}^{60}\underline{E}^{61}$F (Domain 1), GF^{167}G^{168}F to G$\underline{R}^{167}\underline{E}^{168}$F (Domain 2), G^{271}FR^{273}F^{274} to $\underline{K}^{271}$F$\underline{R}^{273}\underline{E}^{274}$ (Domain 3), and SYG^{413}F^{414} to SY$\underline{R}^{413}\underline{E}^{414}$ (Domain 4), were generated by QuikChange™ site-directed mutagenesis using pCMVTag2C:IKEPP or pACT2:IKEPP as templates and the primer pairs shown in **Supplemental Table 1**. Mutations were designed to disrupt PDZ ligand-binding at each domain solely through destabilization of the hydrophobic binding pocket of each PDZ domain, and were validated through the use of the online protein domain organization tool, Pfam [43]. All mutations were confirmed by DNA sequence analysis.

2.3. Yeast-2-hybrid screening and yeast matings

Yeast-2-hybrid (Y2H) screening of a human kidney cDNA library (Clontech; 3.5 X 10^6 independent clones; HY4043AH) with the carboxyl-terminal (C-tail) domain, encoding amino acids 299 – 386, of the hIP (hIP$^{299\text{-}386}$) as specific bait was carried out as previously described [33, 34]. Y2H screening identified several independent clones encoding amino acids 1-287 of IKEPP, expressed in the yeast prey plasmid pACT2:IKEPP, as an interactant of the hIP. pGBKT7, pGBKT7:p53, encoding the yeast GAL4 DNA

binding domain (DBD) alone or as a fusion with p53, and pTDI, encoding the SV40 large T antigen as a fusion with the GAL4 activation domain (AD), were obtained from Clontech. All yeast protocols were standard procedures as previously described [34, 38]. For all Y2H-based studies, the interaction of p53, encoded by pGBKT7:p53, with its known interactant the SV40 large T antigen, encoded by pTDI, was routinely used as an internal positive control while the absence of an interaction of p53 with IKEPP, or its derivatives, was used to confirm that no non-specific interactions occurred.

2.4. Cell Culture and transfections

Human embryonic kidney (HEK) 293 cells were obtained from American Type Culture Collection (ATCC) and grown in minimal essential medium (MEM) containing 10 % foetal bovine serum (FBS). HEK 293 cells were transiently or stably transfected using the calcium phosphate/DNA co-precipitation or Effectene® procedures, as previously described [34, 44]. In brief, approximately 48 hr prior to transfection, cells were routinely plated at a density of 2 X 10^6 cells per 10 cm culture dish in 8 ml media. Thereafter, cells were transiently co-transfected with pcDNA, pHM6 or pCMV-based vector in the presence of pADVA [45] at a ratio of 2.5 : 1 using either the calcium phosphate/DNA co-precipitation procedure, where a total of 35 µg DNA was used, or the Effectene® (Qiagen) transfection procedure, where a total of 2 µg DNA was used. HEK.hIP, HEK.hIP^{SSLC}, HEK.hIP$^{\Delta 383}$ cells stably over-expressing HA-tagged forms of the wild type and mutated hIPs, respectively, have been described [32].

The immortalized human kidney (HK-2) cells, obtained from the ATCC, were maintained in 1:1 Delbecco's modified Eagle's medium (DMEM):Hams F-12 (Promocell) supplemented with insulin (5 µg/ml), transferrin (5 µg/ml), sodium selenite (5 ng/ml), hydrocortisone (36 ng/ml), epidermal growth factor (EGF) (10 ng/ml), tri-iodothyronine (4 pg/ml), 2 mmol/l glutamine, and 100 U/ml penicillin and 100 µg/ml streptomycin. The colonic epithelial Caco-2 cells were cultured with DMEM high-glucose medium supplemented with 10% FCS. Human endothelial EA.hy926 cells, obtained from the Tissue Culture Facility at UNC Lineberger Comprehensive Cancer Centre, Chapel Hill, NC, were cultured in Dulbecco's modified Eagle's medium (DMEM), 10% FBS [46]. Primary (1^o) human umbilical vein endothelial cells (HUVECs), obtained from Lonza (IRT9-048-0904D), were routinely cultured in M199 media (Sigma-Aldrich) supplemented with 0.4 % (v/v) Endothelial Cell Growth Supplement/Heparin (ECGS/H; Lonza), 20 % (v/v) FBS and 0.2 % (v/v) L-glutamine. 1^o HUVECs were used between passages 2 - 8. All mammalian cells were grown at 37 ^oC in a humid environment with 5 % CO_2 and confirmed to be mycoplasma free.

2.5. Immunoprecipitations

HEK.hIP, HEK.hIP^{SSLC} and HEK.hIP$^{\Delta 383}$ cells were transiently co-transfected with pADVA and pCMVTag2C:IKEPP using Effectene®. To assess the effect of the farnesyl transferase inhibitors (FTIs) R115777 and SCH66336 on the interaction between the hIP and IKEPP, HEK.hIP cells, transiently co-transfected with pCMVTag2C:IKEPP, were incubated 24 hr post-transfection with R115777 and SCH66336 at concentrations indicated in the figure legends or, as a control, with 0.1 % DMSO (vehicle) for 24 hr at 37 °C prior to immunoprecipitation. The effect of the IP-selective agonist, cicaprost, on the association of IKEPP with the hIP and the IP-mediated phosphorylation of IKEPP were examined in HEK.hIP cells, transiently co-transfected with pCMVTag2C:IKEPP, whereby cells were pre-incubated with either vehicle or RO1138452 (10 µM; 10 min) prior to cicaprost stimulation, as indicated. To assess the effect of the kinase inhibitors, H-89 and Gö6983, on the interaction between the hIP and IKEPP, HEK.hIP cells, transiently co-transfected with pCMVTag2C:IKEPP, were incubated 48 hr post-transfection with H-89 and Gö6983 at concentrations indicated in the figure legends or, as a control, with 0.1 % DMSO (vehicle) for 10 min at 37 °C prior to immunoprecipitation or stimulation with cicaprost as indicated. Primary (1 °) HUVECs were plated onto 10 cm dishes to achieve > 80 % confluence. In all cases prior to immunoprecipitation, cells were washed in the appropriate serum-free media and either incubated with vehicle or with 1 µM cicaprost for the times indicated in the figure legends. Thereafter, cells were washed, lysed and clarified as per previously detailed protocols [33, 34]. HA-tagged forms of the hIP, $PGF_{2\alpha}$ receptor (FP) or EP_3-subtype of the PGE_2 receptor (EP) were immunoprecipitated using *anti*-HA (101R; 1 : 300) antibody; FLAG-tagged IKEPP was immunoprecipitated with *anti*-FLAG M2 (1 : 200); endogenously expressed hIP was immunoprecipitated with the affinity purified rabbit polyclonal *anti*-hIP (1 : 50) antibody [33] or, as negative controls, with normal rabbit IgG (Santa Cruz). Thereafter, lysates were incubated for 1 hr with either a 50 % slurry of protein G-sepharose (10 µl) or protein A-sepharose (10µl) prior to repeated washing with radioimmune precipitation buffer (RIP; 50 mM Tris-Cl, pH 8.0, 150 mM NaCl, 1 mM EDTA, 1% Nonidet P-40 (v/v), 0.5% sodium deoxycholate (w/v), 0.1% SDS (w/v), 10 mM sodium fluoride, 25 mM sodium pyrophosphate,

1 μg/ml leupeptin, 0.5 mM phenylmethylsulfonyl fluoride and 1 mM sodium orthovanadate) followed by PBS (2 - 3 times). Immunoprecipitates were resolved by SDS-PAGE and subjected to immunoblotting with either *anti*-FLAG (1 : 1000), *anti*-HA (3F10; 1 : 500), *anti*-IKEPP (1 : 500), *anti*-HDJ-2 (1 : 4000), and/ or *anti*-PhosphoSer (1 : 1000) antibodies, as indicated.

2.6. Immunohistochemistry

Normal human kidney tissue blocks, formalin-fixed and paraffin-embedded, were obtained through ethical consent from St Vincent's University Hospital, Dublin, Ireland. Tissue sections were cut at 4 μm thickness and baked onto slides at 50 - 56 °C for up to 60 min. Prior to immunolabelling, sections were dewaxed in two changes of xylene (2 × 10 min) and rehydrated through a series of decreasing alcohol solutions (100%, 5 min x 2; 95 %, 1 min; 80 %, 1 min) before being washed in distilled water. Endogenous peroxidase activity was blocked by incubating the tissue sections in 3 % hydrogen peroxide, prepared in methanol, for 10 min at room temperature, followed by repeated washing of slides in PBS. Thereafter, non-specific binding was blocked by incubating the tissue sections for 30 min at room temperature with 1 % horse serum in PBS (Blocking buffer) to which Avidin D (4 drops per ml of blocking buffer; Vector Labs Avidin/Biotin Blocking kit) was added to block endogenous biotin. Sections were then incubated with primary (1 °) antibody, prepared in blocking buffer and containing Biotin (4 drops per ml of blocking buffer; Vector Labs Avidin/Biotin Blocking kit), where rabbit *anti*-hIP [33] and rabbit *anti*-IKEPP (Abcam®) antibodies were used at 10-12 μg/ml. Following overnight incubation at 4 °C in a humidified chamber with the primary antibodies, sections were washed in PBS, prior to incubation for 30 min with biotinylated universal secondary antibody (1 : 50 dilution; Vectastain Universal Elite ABC kit), prepared in blocking buffer. After washing, tissue sections were incubated with Vectastain ABC reagent, as per manufacturer's instructions, followed by incubation of tissue sections with the chromogen 3,3'-diaminibenzidine (DAB) substrate (0.05 % DAB, 0.015% hydrogen peroxide in PBS) for 5 - 10 min. Tissue sections were counterstained with haemotoxylin, dehydrated through increasing alcohol series and xylene (2 × 10 min) prior to mounting in DPX. Slides were imaged using a Zeiss microscope and Axiovision software.

2.7. Immunofluorescence Microscopy

To examine the localization of IKEPP and the hIP, HEK.hIP cells transiently co-transfected with pCMVTag2C:IKEPP plus pADVA were grown on poly-L-lysine treated coverslips in 6-well plates for at least 48 hr post-transfection. Thereafter, essentially as previously described [38], cells were fixed and permeabilized prior to immunolabelling with the affinity purified rabbit polyclonal *anti*-hIP antibody (1 : 500; 1 % BSA in TBS) or *anti*- IKEPP (1 : 500; 1 % BSA in TBS) for 1 hr at RT followed by AlexaFluor488 goat *anti*-rabbit IgG secondary antibody (1 : 2000; 1 % BSA in TBS) or AlexaFluor594 rabbit *anti*-mouse IgG secondary antibody (1 : 4000; 1 % BSA in TBS), to detect the IP receptor or IKEPP respectively. Imaging was carried out using the Zeiss Axioplan 2 microscope and Axioplan Version 4.4 imaging software. Data presented are representative images of at least three independent experiments from which at least 10 fields were viewed at 63X magnification, where the horizontal bar represents 10 μM.

2.8. Radioligand Binding Assays

To examine the effect of IKEPP on hIP expression, HEK.hIP cells were transiently co-transfected with pCMVTag2C:IKEPP in the presence of pADVA or, as a control, with pCMVTag2C. Radioligand binding assays (RLBAs; saturation binding studies and Scatchard analyses) of the hIP were carried out as previously described [31, 38].

2.9. Measurement of agonist-induced cAMP generation

A gene reporter-based assay was performed to investigate the effect of over-expression of IKEPP on changes in intracellular cAMP levels in response to stimulation of the hIP with its selective agonist cicaprost, essentially as previously described [47]. In brief, the plasmids pHM6:hIP (1.5 μg), pCMVTag2C:IKEPP (2 μg), pCMVTag2C:IKEPP^{PDZD1*} (2 μg), pCMVTag2C:IKEPP^{PDZD2*} (2 μg), pCMVTag2C:IKEPP^{PDZD3*} (2 μg), pCMVTag2C:IKEPP^{PDZD4*} (2 μg) or, as a negative control, pCMVTag2C, were each transiently co-transfected into HEK 293 cells with the luciferase reporter pCRE-Luc (1 μg), pRL-TK (50 ng) and pADVA (0.5 μg) using Effectene® reagent as per the manufacturers' instructions (Qiagen). Cells were treated 72 hr post-transfection with 3-isobutyl-1-methylxanthine (IBMX; 100 μM) at 37 ^{o}C for 30 min and then stimulated with either vehicle (V; 0.01 % DMSO) or 1 μM cicaprost at 37 ^{o}C for 3 hr. Firefly and renilla luciferase activity was assayed 76 hr post-transfection using the Dual Luciferase Assay System®. Relative firefly to

renilla luciferase activities (arbitrary units) were calculated as a ratio and were expressed in relative luciferase units (RLU).

2.10. Disruption of IKEPP expression by small interfering (si)RNA

For small interfering (*si*) RNA experiments, 1° HUVEC cells were plated at ~2.5 x 10^5 cells /35 - mm plate and some 24 hr prior to transfection such that cells reach ~50 % confluence. Thereafter, cells were transfected with 30 nM IKEPP *si*RNA (*si*RNA_{IKEPP}; 5'-GCAAGUGGGAGACGUGAUUtt-3'; Dharmacon), 30 nM Lamin A/C *si*RNA (*si*$RNA_{LaminA/C}$; 5'-CUGGACUUCCAGAAGAACAtt; Qiagen) or 30 nM scrambled negative control *si*RNA (*si*$RNA_{CONTROL}$; 5'-AATTCTCCGAACGTGTCACGTtt-3'; Qiagen) using RNAiFECT transfection reagent (Qiagen), as per manufacturer's instructions. To confirm the efficacy of the *si*RNA to disrupt IKEPP expression, following transfection 1° HUVECs were harvested after incubation at 0 – 72 hr and subject to SDS-PAGE (10 – 15 µg/lane on 10 % polyacrylamide gels) followed by electroblotting onto PDVF membranes (Roche). Membranes were successively screened using *anti*-IKEPP (1 : 1000 dilution; Santa Cruz) and *anti*-Lamin A/C (1 : 500 dilution; Santa Cruz) antibodies and then screened using *anti*-HDJ-2 (1 : 4000 dilution; Neomarkers) antibody to confirm uniform protein loading. For migration and tube formation assays, 24 hr post-*si*RNA transfection cells were placed in reduced serum growth media (2.5 % FBS) for 16 hr before experiments were performed.

2.11. Cell Migration assays

In order to monitor changes in 1° HUVEC migration, scratch wound assays were performed essentially as previously described [38] where cells were pre-incubated with either vehicle (0.01 % PBS), cicaprost (1 µM) or VEGF (50 ng/ml) and wound closure assessed 12 hr post-injury. Reduction in scratch paths were visualized and imaged using a Nikon TMS inverted microscope with Matrox Intellicam software (Version 2.07) and analysed with TScratch software (Version 1.0). Migration was expressed as mean (± S.E.M.) percentage of basal cell migration, where at least three independent experiments were performed in triplicate.

2.12. In Vitro Tube Formation Assays

Matrigel tube formation assays were performed to assess *in vitro* angiogenesis essentially as previously described [38] where tube formation in 1° HUVECs stimulated with either vehicle (0.01 % PBS), cicaprost (1 µM) or VEGF (50 ng/ml) was examined. After 12 hr incubation, cell morphology was visualized and imaged at 40X magnification using a Nikon TMS inverted microscope with Matrox Intellicam software (Version 2.07; 4 times at random per field). The length of tube was measured with WCIF ImageJ software (Version 1.37c) and expressed as mean (± S.E.M.) percentage of basal tube length, where at least three independent experiments were performed in triplicate.

2.13. Data analyses

Statistical analyses of differences were carried out using 1-way or 2-way ANOVA followed by post-hoc Dunnett's multiple comparison *t* tests, as indicated, throughout employing GraphPad Prism, version 4.00 package. *P*-values of less than or equal to 0.05 were considered to indicate a statistically significant difference. As relevant, single, double and triple symbols signify $p \leq 0.05$, ≤ 0.01 and ≤ 0.001, respectively, for post-hoc Dunnett's multiple comparison *t*-test analyses.

3. RESULTS

3.1. Identification of IKEPP as an interactant of the hIP

We recently identified Rab11a [33, 34] and PDZK1 [38] as GPCR interacting proteins/GIPs that directly and specifically interact with the hIP involving unique binding domains within its proximal and distal C- tail region, respectively. While Rab11a binds to a 14-residue Rab11a binding domain (RBD), comprising Val^{299}-Val^{307} and adjacent to the palmitoylated residues Cys^{308}-Cys^{311}, located within the proximal C-tail domain of the hIP [33], the interaction of PDZK1 is dependent on the three C-terminal residues of the hIP corresponding to a class I PDZ ligand [38]. Herein, we report the identification of Intestinal and Kidney Enriched PDZ Protein (IKEPP), the fourth member of the Na^+/H^+ exchange regulatory factor (NHERF) family of intracellular multi-PDZ domain adaptor proteins, as a direct interacting partner of the hIP. Specifically, using the C-tail domain ($hIP^{299-386}$) of the hIP as the initial bait protein, yeast-two-hybrid (Y2H) screening of a human kidney cDNA library identified several independent clones encoding amino acids 1-287 of IKEPP ($IKEPP^{1-287}$), encompassing its entire PDZ domains 1 (PDZ^{D1}) and 2 (PDZ^{D2}; **Figure 1A)** as interactants of the hIP.

To further characterize the interaction, extended Y2H matings were performed using $IKEPP^{1-287}$ and various subfragments derived from the C-tail domain of either the wild-type ($hIP^{299-386,WT}$ or $hIP^{320-386,WT}$), the isoprenylation-defective ($hIP^{299-386,SSLC}$) forms of the hIP, or a subfragment corresponding to the RBD of the hIP ($hIP^{299-320}$) alone (**Figure 1A**). While each of the bait and prey strains mated successfully to form diploids (**Figure 1A,** DDO), $IKEPP^{1-287}$ only interacted with the subfragments containing the C-terminal residues of the hIP domain ($hIP^{299-386}$ & $hIP^{320-386}$; **Figure 1A**, QDO). Conversely, $IKEPP^{1-287}$ did not interact with the $hIP^{299-320}$ fragment (**Figure 1A,** QDO) or with any of the controls proteins, including p53 or that encoded by the vector alone (**Figure 1A**, QDO). Furthermore, the interaction of $IKEPP^{1-287}$ with the hIP subfragments was independent of the presence of an isoprenylation 'CaaX' motif associated with the wild type hIP (-C^{383}SLC; *e.g.,* in $hIP^{299-386,WT}$ or $hIP^{320-386,WT}$) or an isoprenylation-deficient variant associated with the hIP^{SSLC}(-S^{383}SLC; *e.g.,* in $hIP^{299-386,SSLC}$). These data confirm that $IKEPP^{1-287}$ specifically interacts with the C-tail domain of the hIP.

Thereafter, the ability of full-length IKEPP ($IKEPP^{1-505}$, hereinafter referred to as IKEPP) to specifically interact with hemagglutinin (HA)-epitope tagged forms of either the wild-type hIP, hIP^{SSLC} or $hIP^{\Delta 383}$ expressed in the previously characterized mammalian HEK.hIP, HEK.hIP^{SSLC}, and HEK.$IP^{\Delta 383}$ cell lines [32] was examined through co-immunoprecipitation studies (**Figure 1B**). FLAG-tagged IKEPP was detected in *anti*-HA immunoprecipitates from cells expressing either the wild type hIP or isoprenylation-deficient hIP^{SSLC} and at similar levels in both cases (**Figure 1B**, upper panel). In contrast, only trace amounts of IKEPP was co-immunoprecipitated with the $hIP^{\Delta 383}$, a variant of the hIP lacking the extreme C-terminal amino acids including its entire CaaX box (**Figure 1B,** upper panel). Furthermore, IKEPP was not detected in the *anti*-HA:FP or *anti*-HA:EP_3 immunoprecipitates from the control HEK 293 cell lines over-expressing HA-tagged forms of the prostaglandin $(PG)F_{2\alpha}$ receptor (the FP) or the EP_3 subtype of the PGE_2 receptor (**Figure 1C**, upper panel). Such differences in co-immunoprecipitation of IKEPP with the various HA-tagged receptors used were not due to failure or variations in the immunoprecipitations *per se* (**Figures 1B & 1C,** middle panels) or due to differences in the levels of FLAG-tagged IKEPP expressed in the cell lysates employed in the individual immunoprecipitations (**Figures 1B & 1C,** lower panels).

To further investigate the possible influence of the isoprenylation status of the hIP on its interaction with IKEPP, the effect of inhibition of farnesylation of the hIP following incubation of HEK.hIP cells with the selective farnesyl transferase inhibitors (FTIs) R115777 or SCH66336 was examined (**Figure 1D,** upper panel). As controls for these studies, the ability of the FTIs to inhibit general protein farnesylation was confirmed whereby both agents efficiently inhibited farnesylation of the molecular chaperone protein HDJ-2, as evidenced by the presence of the non-farnesylated (49 kDa) in addition to the farnesylated (45 kDa) species of HDJ-2 in the presence of the FTIs while only the farnesylated species was present in their absence (**Figure 1C,** lower panel). Neither R115777 nor SCH66336 treatment affected the level of IKEPP co-immunoprecipitated with the hIP (**Figure 1D**, upper panel).

Taken together, these data identify a novel interaction between IKEPP and the hIP in both yeast and mammalian cells. Furthermore, while the interaction requires the presence of the C-terminal residues of the hIP, it appears to be independent of the isoprenylation status of the hIP *per se*.

3.2. Characterization of the PDZ ligand and identification of the PDZ interacting domains.

PDZ ligands at the extreme C-termini of target proteins typically belong to one of three Classes I-III, depending on the sequence composition of the 3 terminal residues [3]. Through its interaction with PDZK1, the C-terminal residues of the hIP were previously identified as a Class I PDZ ligand, with the typical

Ser/Thr-X-Φ-COOH consensus sequence [38]. Herein, Y2H-based interaction studies were used to re-examine the PDZ ligand determinants of the hIP involved in its interaction with IKEPP$^{1-287}$. To this end, the importance of residues at the P_0, P_{-1}, P_{-2}, and P_{-3} of the PDZ ligand involved in the interaction of the hIP with IKEPP$^{1-287}$ was investigated by mutation of those residues to corresponding Ser or Ala residues, either alone or in combination (**Figure 2A**).

As previous, each of the bait and prey strains mated successfully to form diploids (**Figure 2A,** DDO panels). Specific mutations of the hIP at the P_{-1} (hIP$^{299-386,CS\underline{A}C}$, a variant not predicted to be isoprenylated, or hIP$^{299-386,CS\underline{S}C}$, a variant predicted to be isoprenylated) and at the P_{-3} positions (hIP$^{299-386,\underline{S}SLC}$) did not affect their ability to interact with IKEPP$^{1-287}$. Conversely, mutation at the P_0 (hIP$^{299-386,CSL\underline{S}}$) abolished the interaction, whereas mutation at the P_{-2} (hIP$^{299-386,C\underline{A}SC}$) substantially reduced the interaction with IKEPP (**Figure 2A,** QDO panels). Moreover, combined mutation of the $P_{0,\,-1,\,-2}$ (hIP$^{299-386,C\underline{AAA}}$), $P_{0,\,-1,\,-2,\,-3}$ (hIP$^{299-386,\underline{S}AAA}$) or deletion of $P_{0,\,-1,\,-2}$ (hIP$^{299-386,C\text{-stop}}$ or hIP$^{299-386,S\text{-stop}}$) generated forms of the hIP that did not interact with IKEPP. Collectively, these data reaffirm that the C-terminal residues of the hIP act as a Class I PDZ ligand, where the C-terminal Cys^{386} at P_0 and Ser^{384} at P_{-2} are obligate for its interaction with IKEPP and data herein is in complete agreement with that previously obtained from studies involving the interaction of the hIP with PDZK1 [38].

Similar to PDZK1, IKEPP is a member of the NHERF family containing 4 PDZ domains, referred to hereinafter as PDZ^{D1}, PDZ^{D2}, PDZ^{D3} and PDZ^{D4} (**Figure 2B**). While the original Y2H screen initially identified IKEPP$^{1-287}$, comprising PDZ^{D1} and PDZ^{D2}, as the specific interactant of the hIP, it was sought to establish whether PDZ^{D1} and/or PDZ^{D2} or indeed whether the other PDZ^{D3} and/or PDZ^{D4} domains may also contribute to the interaction with the hIP. To this end, the Y2H-based approach was used to examine the interaction of the hIP$^{299-386}$ and its derivatives, as listed, with subfragments of IKEPP encoding its individual PDZ^{D1}, PDZ^{D2}, PDZ^{D3}, PDZ^{D4} or combined PDZ^{D1-D2} domains (**Figure 2B & 2C**). Only subfragments of IKEPP containing PDZ^{D1}, namely PDZ^{D1} alone or PDZ^{D1-D2}, showed a specific interaction with the hIP derivatives (hIP$^{299-386\ WT}$, hIP$^{299-386\ SSLC}$ & hIP$^{320-386\ WT}$) while the PDZ^{D2}, PDZ^{D3} or PDZ^{D4} subfragments failed to show any interaction (**Figure 2C**, QDO). Furthermore, as expected, none of the PDZ domains of IKEPP interacted with the RBD of the hIP (hIP$^{299-320}$) or with other control proteins, including p53 or that encoded by the vector alone (**Figure 2C**, QDO). These data suggest that PDZ^{D1} plays a critical role in the interaction of IKEPP with the hIP.

The folding pattern of domains within proteins, in particular in those with multiple domains, may be influenced by the presence of those other domains [48]. Hence, it is theoretically possible that failure to observe an interaction between the PDZ ligand of the hIP with the individual PDZ^{D2}, PDZ^{D3} or PDZ^{D4} domains of IKEPP may simply be due to altered folding or indeed due to misfolding. Hence, as an additional, independent means of identifying the PDZ domain(s) of IKEPP involved in its interaction with the hIP, the effect of mutation of the critical residues within the 'GLGF' motif of the carboxylate binding loop (CBL)/hydrophobic binding pocket of each of the individual PDZ^{D1}, PDZ^{D2}, PDZ^{D3} or PDZ^{D4} domains on the interaction of full length IKEPP with the PDZ ligand of the hIP was investigated (**Figure 3A & 3B**). Consistent with previous data (**Figure 2C**), mutation of the 'GLGF' motif in PDZ^{D1} completely abolished the interaction of IKEPP^{PDZD1*} with all the hIP subfragments containing a functional PDZ ligand (**Figure 3B**, QDO). Conversely, mutation of the 'GLGF' motifs in PDZ^{D2} (IKEPP^{PDZD2*}), PDZ^{D3} (IKEPP^{PDZD3*}) or PDZ^{D4} (IKEPP^{PDZD4*}) did not affect the interaction (**Figure 3B**, QDO). Furthermore, specific mutation of the 'GLGF' motifs within the individual PDZ^{D1} and PDZ^{D2} domains present in IKEPP$^{1-287}$, the original Y2H interactant, confirmed that disruption PDZ^{D1}, but not PDZ^{D2}, abolished the interaction with the PDZ ligand of the hIP (data not shown).

As an additional means of identifying the PDZ domain(s) involved in the interaction, the effect of mutating the 'GLGF' motifs within the individual PDZ^{D1}, PDZ^{D2}, PDZ^{D3} or PDZ^{D4} domains on the interaction of full length IKEPP with the hIP expressed in mammalian HEK 293 cells was investigated through co-immunoprecipitations. In agreement with previous data (**Figure 1B-1D**), IKEPP co-precipitated in immune-complexes with the hIP (**Figure 3C**, upper panel). Disruption of the 'GLGF' motif within PDZ^{D1*} ($p < 0.001$) and, to a lesser extent, within PDZ^{D2*} ($p < 0.05$) led to significant reductions in the interaction of IKEPP with the hIP as evidenced by the reduced level of IKEPP present in the *anti*-HA:hIP immune complexes (**Figure 3C**, upper panel). Conversely, disruption of the 'GLGF' motifs within PDZ^{D3*} or PDZ^{D4*} did not affect the interaction of IKEPP with the hIP (**Figure 3C**, upper panel). Any differences in levels of IKEPP in the immune-complexes was not due variations in levels of precipitation of the hIP *per se*, or indeed due to differences in the expression of IKEPP or its derivatives in the cell lysates (**Figure 3C,** middle and lower panels, respectively).

Collectively these data confirm that hIP contains a Class I PDZ ligand at its C-terminus and identify a critical role for PDZ^{D1} and, to a lesser extent, for PDZ^{D2} of IKEPP in the interaction with the hIP.

3.4. Effect of IKEPP on the Expression and Signalling of the hIP

PDZ containing proteins, including IKEPP, have been shown to affect the expression and/or function of certain of their targets, and in a protein and/or cell type-specific manner [7, 10, 13, 49]. Having established that IKEPP acts as a direct interactant of the hIP, its effect on the expression and signalling of the hIP in the clonal HEK.hIP cell line was investigated. Although immunoblot analysis suggested that ectopic expression of IKEPP did not affect the overall level of hIP expression *per se* in HEK.hIP cells (**Figure 4A**, IKEPP; $P = 0.70$), saturation radioligand binding assays showed that over-expression of IKEPP led to a 1.7-fold increase in binding of the IP radioligand [^{3}H]iloprost in crude membrane preparations (**Figure 4A**, IKEPP; $P < 0.01$). Furthermore, Scatchard analysis established that expression of IKEPP led to an ~ 2-fold increases in maximal Iloprost binding (Bmax) by the hIP without affecting the binding affinity (Kd) *per se* (2.08 ± 0.72 nM, $P < 0.72$, high affinity binding site; 24.45 ± 0.50, $P < 0.40$, low affinity binding site; [50]), suggesting that IKEPP may be enhancing the expression of functionally mature hIP, rather than increasing its overall expression. These findings were corroborated by flow cytometric analysis whereby it was established that the relative fluorescence intensity due to *anti*-HA hIP analysis was unaltered in the presence of IKEPP compared to control cells (**Supplemental Figure 1A**). This is in direct contrast with that of the control protein PDZK1 which, in agreement with previous reports [38], led to ~ 1.4 fold increase in expression of the hIP (**Supplemental Figure 1A**). Furthermore, the level of hIP -induced cAMP generation in response to stimulation with the selective agonist cicaprost was significantly increased in HEK.hIP cells following over-expressing IKEPP compared to control cells (**Figure 4B**; $P < 0.001$). Collectively, these data suggest that ectopic expression of IKEPP leads to an increase in the expression of functionally active hIP, without affecting its overall expression levels *per se*.

As a means of validating that such effects of IKEPP are due to a PDZ-domain type interaction with the hIP, the effect of disruption of the 'GLGF' motif in each of the individual PDZ domains of IKEPP on [^{3}H]iloprost binding and cicaprost-induced cAMP generation by the hIP expressed in HEK.hIP cells was investigated. Disruption of the 'GLGF' motif in PDZ^{D1} ($IKEPP^{PDZD1*}$) completely abolished the IKEPP-induced increase in both radioligand binding (**Figure 4C**) and cicaprost-induced cAMP generation (**Figure 4D**) by the hIP. Moreover, disruption of the 'GLGF' motif in PDZ^{D2} ($IKEPP^{PDZD2*}$) also reduced the increase in both [^{3}H]iloprost binding and cicaprost-induced cAMP generation, albeit to a lesser extent than with $IKEPP^{PDZD1*}$ (**Figure 4C & D**). In contrast, disruption of the 'GLGF' motifs in either PDZ^{D3} or PDZ^{D4} did not have a significant effect on the IKEPP-induced increases in either radioligand binding or cAMP generation by the hIP (**Figure 4C & D**). Hence, taken together, these data confirm that IKEPP leads to an increase in the functional expression of the hIP and provide further evidence that PDZ^{D1}, and to a lesser extent PDZ^{D2}, are the PDZ domains responsible for mediating the interaction between IKEPP and the hIP in mammalian cell lines.

3.5. Effect of Agonist-activation of the hIP on its Interaction with IKEPP

To investigate the possible influence of agonist activation of the hIP on its interaction with IKEPP, the effect of cicaprost-stimulation was examined through co-immunoprecipitations in HEK.hIP cells. Consistent with previous data (**Figure 1B - 1D**), in the absence of agonist, IKEPP was readily detected in immune-complexes with the *anti*-HA.hIP (**Figure 5A**, upper panel). In response to cicaprost stimulation, the level of IKEPP in the *anti*-HA.hIP immunoprecipitates was significantly increased (**Figure 5A**, upper panel; 1 μM, 10 min; $p = 0.0079$), an effect that was abrogated by the pre-incubation of HEK.hIP cells with the highly specific IP antagonist RO1138452 (**Figure 5A**, upper panel; 10 μM, 10 min). Such differences in the levels of IKEPP in the *anti*-HA.hIP immunoprecipitates were not due differences in the efficiency of the immunoprecipitation *per se* (**Figure 5A;** middle panel) or due to substantial differences in IKEPP expression in the cell lysates (**Figure 5A;** lower panel).

Many PDZ domain-containing proteins, including IKEPP and other members of the NHERF family are phosphoproteins and, in several cases, phosphorylation is thought to play a role in regulating the interaction of the PDZ domain protein with its given target(s) [5, 51, 52]. Furthermore, somewhat similar to that observed herein involving IKEPP, the interaction of the hIP with PDZK1/NHERF3 has also been established to be regulated in an agonist-dependent manner and, more specifically, this regulated interaction occurs through a mechanism involving direct IP-induced cAMP-dependent protein kinase (PK)A-phosphorylation of PDZK1 at Ser^{505} [38]. Hence, to investigate if the agonist-regulated interaction of IKEPP with the hIP may actually involve alterations in the phosphorylation status of IKEPP, the effect of cicaprost

stimulation on the phosphorylation of IKEPP was investigated employing an *anti*-Phospho^{Ser} -specific antibody (**Figure 5B**). Under basal conditions, in the absence of agonist, the level of phospho^{Ser} detected in the *anti*-FLAG:IKEPP immunoprecipitates was minimal (**Figure 5B**, upper panel). In response to cicaprost stimulation of the hIP (1 μM, 10 min), there was a substantial increase in IKEPP phosphorylation as evidenced by increased level of phospho^{Ser} detected in the *anti*-FLAG:IKEPP precipitates (**Figure 5B**, upper panel, $p < 0.0001$). Confirmation that the enhanced cicaprost-induced phosphorylation of IKEPP is mediated through activation of the hIP was established whereby the selective IP antagonist RO1138452 impaired the cicaprost-induced phosphorylation of IKEPP (**Figure 5B**, upper panel, $p = 0.002$). Furthermore, immunoblotting of the *anti*-FLAG immunocomplexes confirmed that the observed differences in the *anti*-Phospho^{Ser} signal was not due to variations in the efficiency of the immunoprecipitation of IKEPP *per se* (**Figure 5B**, lower panel).

Hence, these data establish that the interaction of IKEPP with the hIP is increased in response to receptor activation, an effect that coincides with increased hIP-dependent phosphorylation of IKEPP. As stated, the hIP is primarily coupled to Gs/adenylyl cyclase and, in turn, to downstream cAMP dependent protein kinase (PK)A activation but can also couple to Gq/phospholipase (PL)Cβ PKC activation [28, 30]. Therefore, in view of the agonist-regulated interaction of IKEPP with the hIP that coincides with the increased hIP-induced phosphorylation of IKEPP, the role of the second messenger-regulated kinases PKA and PKC on the agonist (cicaprost)-regulated interaction of IKEPP was investigated (**Figure 6**). As previous (**Figure 5A**), while IKEPP was found in the *anti*-HA.hIP immunoprecipitates from HEK.hIP cells under basal conditions in the absence of agonist, the levels of IKEPP in the immune-complexes were significantly increased in response to cicaprost stimulation (**Figure 6**, upper panel). Pre-treatment of HEK.hIP cells with either the PKA inhibitor H-89 (10 μM, 10 min) or with the PKC inhibitor Gö6983 (1 μM, 10 min) alone did not affect the level of IKEPP present in the *anti*-HA.hIP immunoprecipitates either in the absence of agonist or following cicaprost-stimulation (**Figure 6**, upper panel). However, while the basal interaction between the hIP and IKEPP was unaffected, pre-incubation with both H-89 and Gö6983 together completely impaired the enhanced cicaprost-induced association of IKEPP in the *anti*-HA.hIP complexes (**Figure 6**, upper panel). In fact, in the presence of H-89 and Gö6983, levels of IKEPP present in the hIP immune-complexes were not significantly different to those levels found in the absence of cicaprost stimulation (**Figure 6**).

Collectively, these data establish that the interaction of the hIP with IKEPP/NHERF4 is modulated by agonist-induced activation of the hIP which occurs, at least in part, through a mechanism involving PKA and PKC-induced phosphorylation of IKEPP.

3.6. Localization of IKEPP and the hIP within the Human Kidney and Vascular Endothelial Cells

IKEPP was originally identified as an interactant of guanylyl cyclase C in a Y2H screen of a human intestinal cDNA library and its expression was subsequently determined to be restricted to the kidney, small intestine and colon [7-9]. Prostacylin has long been known as an important mediator of renal hemodynamics and expression of the hIP has been detected in renal tubules [24, 53, 54]. Herein, in view of the novel interaction of IKEPP with the hIP, it was sought to examine their expression in human kidney tissue sections. Immunohistochemical analysis, using a previously characterized, affinity purified rabbit polyclonal antibody directed to intracellular loop $(IC)_2$ of the hIP [33], confirmed expression of the hIP in both the cortex and medulla regions of the kidney, particularly in the epithelium lining the renal tubules (**Figure 7A & Supplemental 2A;** *anti*-hIP). Likewise, IKEPP was detected in the epithelium lining of the tubules in both regions (**Figure 7A & Supplemental 2A;** *anti*-IKEPP). For example, in the renal cortex, intense immunolabelling of both the hIP and IKEPP was observed in the distal tubules, distinguished by their clear lumen (**Figure 7Ai & Supplemental 2Ai;** upper insets), while in the proximal tubules the staining was less intense (**Figure 7Ai & Supplemental 2Ai;** lower insets). Hence, the hIP and IKEPP localize *in situ* to the same cells within the human kidney.

As stated, prostacyclin and the IP play a critical role throughout the vasculature, including in platelets, smooth muscle and in the vascular endothelium [22]. Hence, having discovered a novel interaction between the hIP and IKEPP, possible expression of IKEPP in cells derived from the vascular endothelium was evaluated and, as a reference, compared to that in cell lines of the renal and GI system where it is widely reported to be expressed. Consistent with previously published data [7, 9], IKEPP is strongly expressed in cellular extracts from the renal HK2 and the intestinal Caco-2 cell lines (**Figure 7B**), where it migrates as a triplet, in keeping with the existence of multiple isoforms of IKEPP [7]. In vascular endothelial cells, abundant expression of IKEPP was observed in both the immortalized human endothelial EA.hy926 cell line and in primary (1°) human umbilical vascular endothelial cells (HUVEC; **Figure 7B**). It was noteworthy, in the latter cell types, IKEPP was predominantly expressed as 2 closely migrating protein

isoforms that appeared to be identical in both endothelial cells types but somewhat distinct from the predominant species present in the HK and Caco-2 cells (**Figure 7B**).

Hence, given the abundant expression of IKEPP in the endothelial cell lines, it was sought to determine if IKEPP may actually co-localize and/or interact with the hIP in 1° HUVECs, a physiologically relevant endothelial cell type. To this end, hIP endogenously expressed in 1° HUVECs was immunoprecipitated, using the *anti*-hIP antibody [33], and the presence of IKEPP in those immune-complexes was investigated. IKEPP was readily detected in the *anti*-hIP, but not from IgG, immunoprecipitates from 1° HUVECs (**Figure 7C**, upper panel), confirming an interaction of IKEPP with the hIP. The failure to detect IKEPP in the IgG precipitates was not due to the lack of IKEPP expression (**Figure 7C**, lower panel). Furthermore, immunocytochemical analysis of hIP and IKEPP expression in 1° HUVECs established that both proteins show substantial co-localization where they are principally expressed at the cell membrane with a small intracellular pool of both proteins localized to the perinuclear area (**Figure 7D**). Specificity of the *anti*-hIP antisera was validated whereby pre-incubation of the antiserum with the antigenic peptide, directed to the IC_2 domain of the hIP, specifically blocked immunodetection of the hIP (**Supplemental Figure 2B**).

Taken together, these data establish that IKEPP and the hIP co-localize in the kidney where they exhibit similar, differential staining of the epithelial cells that line the proximal and distal tubules. Furthermore, it has also been established that IKEPP is abundantly expressed in vascular endothelial cells, where it was found in immune-complexes with the hIP. Collectively, these data identify a novel interaction of IKEPP with the hIP and thereby suggest a possible functional role of the interaction not only in the renal system but also in the vascular endothelium where both proteins co-localize.

3.7. Effect of IKEPP on Agonist-induced Endothelial Cell Migration and Angiogenesis

The hIP has been previously implicated in both endothelial cell migration and angiogenesis [22]. More recently, the hIP was shown to play a critical role in endothelial cell migration and *in vitro* angiogenesis/ tube formation in 1° HUVECs and these effects were greatly influenced by the interaction of the hIP with PDZK1 [38]. Hence, given that PDZK1 and IKEPP are structurally and functionally related proteins coupled with the demonstration herein that IKEPP is both expressed and present in immune-complexes with the hIP in vascular endothelial cells, including in 1° HUVECs, it was sought to investigate a possible functional role of IKEPP on hIP-mediated endothelial cell migration and tube formation. Initially, and consistent with our previous findings [38], stimulation of 1° HUVECs with the selective IP agonist cicaprost and, as a control, with the *pro*-angiogenic mediator vascular endothelial growth factor (VEGF) yielded significant increases in endothelial cell migration (**Figure 8A**) and mean endothelial tube length, a measure of *in-vitro* angiogenesis (**Figure 8C**). To investigate the role of IKEPP in participating in the observed endothelial cell migration and tube formation, *small interfering* RNA (*si*RNA) was used to disrupt its expression in 1° HUVECs. While targeted knockdown of IKEPP had little effect on basal endothelial cell migration or mean tube length, carried out in the presence of the drug vehicle, it almost completely inhibited the cicaprost-induced increases in both cellular processes (**Figure 8B & Figure 8D**; $siRNA_{IKEPP}$). In contrast, disruption of IKEPP only marginally reduced VEGF-mediated cell migration and mean tube length in 1° HUVECs (**Figure 8B & Figure 8D**; $siRNA_{IKEPP}$) while the scrambled control $siRNA_{CTRL}$ had no significant effect on either basal-, VEGF- or cicaprost-induced migration or *in vitro* angiogenesis (**Figure 8B & Figure 8D**; $siRNA_{CTRL}$). Moreover, immunoblot analysis confirmed that in the presence of $siRNA_{IKEPP}$, endogenous expression of IKEPP in 1° HUVECs was reduced by more than 90 % in all experiments (**Figure 8E**).

Hence, consistent with previously reported findings [38], these data reaffirm an essential role for the hIP in promoting endothelial cell migration and angiogenesis/endothelial tube formation *in vitro*. More critically, the data presented herein also establishes, for the first time, a role for IKEPP in mediating both cicaprost/IP-induced endothelial migration and *in vitro* angiogenesis in 1° HUVECs and thereby reveal a clear functional link between the hIP and IKEPP within the vasculature.

4. DISCUSSION

We recently identified an interaction between the hIP and PDZK1, the third member of the NHERF family of multi-PDZ domain proteins [38]. Herein, we report that the hIP also interacts with the NHERF4 family member IKEPP. In both cases, the extreme carboxyl-terminal residues of the hIP were identified as a Class I PDZ ligand [3], where residues at the P_0 (Cys^{386}) and P_{-2} (Ser^{384}) positions of the PDZ ligand are essential for the interactions. However, as stated, the hIP is unusual among GPCRs in that it undergoes farnesylation within its evolutionarily conserved -$C^{383}SLC^{386}$ motif [30, 31] while data herein are consistent with recent findings that this 'Caa*X*' motif also acts as a PDZ ligand [38]. While several lines of evidence indicated that the interaction of the hIP with IKEPP is independent of the isoprenylation status of the receptor, follow-up studies involving more direct biophysical approaches are necessary to ascertain which form(s) of the hIP, whether it be the immature, unprocessed (-CSLC) and/or the farnesylated, fully processed forms, that interacts with IKEPP, including for determination of the relative binding affinities.

The ability of the hIP to bind both PDZK1 and IKEPP is not unusual as several other proteins can bind multiple NHERF family members [4, 10, 12, 55]. Furthermore, while the hIP preferentially binds to PDZ^{D3}, PDZ^{D4} and PDZ^{D1}, but not to PDZ^{D2}, of PDZK1 [38], it binds to PDZ^{D1} and, to a lesser extent, PDZ^{D2} but not to PDZ^{D3} or PDZ^{D4} of IKEPP. These data clearly indicate highly specific structural requirements in determining the molecular interactions of the hIP with PDZK1 and with its related IKEPP. Similarly, the organic cation transporter OCT/OCTN family members, OCTN1 and OCTN2, display different binding preferences for PDZ domains within PDZK1 and IKEPP where both OCTN proteins bind to PDZ^{D1}, PDZ^{D2} and PDZ^{D4} of PDZK1 but bind to PDZ^{D1} and PDZ^{D3} of IKEPP [13, 56, 57]. In the case of OCTN2, in addition to the different structural requirements for its interaction with IKEPP and PDZK1, it has also been established that it may be differentially regulated by the 2 NHERF members whereby IKEPP mediates cell surface stabilization of OCTN2 while PDZK1 acts to increase its cation transport activity [13, 56]. Herein, IKEPP was found to increase the functional expression of the hIP, as evidenced by the enhanced ligand binding and agonist-induced cAMP generation, but did not affect the overall level of hIP expression *per se*. In contrast to this, in the case of PDZK1, it led to substantial increases in hIP expression levels at the cell surface, as well as increasing its functional expression [38]. These data suggest that, similar to that reported for other interactants [13, 56], PDZK1 and IKEPP display clear structural and functional differences in their interaction and regulation of the hIP.

Agonist-activation plays an important role in modulating the signalling pathways of members of the GPCR superfamily through modulation of their interaction(s) with specific GIPs including in the case of the hIP with its GIPs [33, 34, 44]. We recently established that the interaction of the hIP with PDZK1 is also dynamically regulated in response to receptor activation and that this occurs through a mechanism involving hIP-mediated cAMP-dependent PKA phosphorylation of PDZK1 at Ser^{505}, within its C-terminal regulatory region [38]. Herein, it was established that IKEPP interacts constitutively with the hIP but that, at 10 min post-agonist activation, this interaction is substantially increased which coincides with increased hIP-induced phosphorylation of IKEPP on Ser residue(s). Furthermore, while inhibition of the second-messenger kinases PKA or PKC alone did not affect the cicaprost-regulated interaction, inhibition of both kinases together completely abrogated the enhanced agonist-induced interaction of IKEPP with the hIP. The suggestion that IKEPP may be phosphorylated at multiple sites by more than one kinase is not without precedence. Within the NHERF family, while NHERF2 is not phosphorylated [4] and PDZK1 is only known to be phosphorylated at Ser^{505} [51], multiple phosphorylation events have been identified for NHERF1 [58]. For example, NHERF1 is phosphorylated by both PKA and PKC even though it is devoid of canonical PKA or PKC phosphorylation motifs [59]. Moreover, it is phosphorylated by PKC and other kinases to modulate its oligomerization and influence its protein complex formation [5]. While our studies suggest that IKEPP may be phosphorylated at Ser residue(s) by both PKA and PKC in response to agonist-activation of the hIP, they do not identify the specific phosphorylated residues nor do they exclude the possibility that other kinase(s) and/or phospho-targeted residue(s), such as at Thr or Tyr, may also be involved. None the less, as stated, inhibition of both PKA and PKC together completely impaired the enhanced agonist-induced interaction of IKEPP with the hIP suggesting key roles for those second messenger-regulated kinases in the modulated interaction. While efforts involving bioinformatics along with mutational studies were made herein to pin-point the actual residues within IKEPP that are phosphorylated in response to hIP activation, owing to the very many potential phospho-target sites that occur within IKEPP, it was not possible to categorically identify those target sites (data not shown). Consistent with this, Thelin *et al.* have evidence of at least 6 potential phosphorylation sites within IKEPP [5]. Hence, additional studies are required to identify the target sites of phosphorylation and to investigate the true implications of the regulated IKEPP interaction for

hIP function including consideration of dynamic interactions following more prolonged agonist-stimulation [38].

IKEPP was originally identified in the kidney and also found in the small intestine and colon but, to our knowledge, its expression has not been detected in any other tissue types to date [5, 7, 8]. Through its regulation of key interacting partners, IKEPP has roles in the renal and gastrointestinal systems in anion secretion [7], calcium secretion [9] and carnitine transport [56]. As stated, prostacyclin is widely implicated in the regulation of renal hemodynamics and expression of the hIP has been detected in renal tubules of the inner and outer medulla and of the cortex [24, 25, 53]. Furthermore, prostacyclin is increasingly implicated in regulating renin release and in the development of renovascular hypertension-associated with obstructive vascular disease, including atherosclerosis [17, 60-62]. Herein, we demonstrate that IKEPP and the hIP colocalize to the epithelial lining of the distal and, to a lesser extent, the proximal renal tubules, pointing to a potential role for the interaction of the hIP with IKEPP in renal hemodynamics. In addition, consistent with the discovery of the expression of the IKEPP in vascular endothelial cells, it was established that it co-localizes with the hIP; is found therein in immune-complexes with the hIP and that, functionally, it plays a key role in hIP-mediated endothelial cell migration and *in vitro* angiogenesis. To the best of our knowledge, this is the first evidence that IKEPP is expressed outside of the renal and gastrointestinal systems and the first indication of a functional role for IKEPP in the vascular endothelium. While our studies were carried out in vascular endothelial cells, it will be of substantial interest to investigate the interplay between IKEPP and the IP within the renal vasculature and whether alterations in that interaction may contribute to the role of the IP in renovascular hypertension-associated with obstructive vascular disease.

Based on data generated herein and from our previous study involving PDZK1 [38], we present a model of the agonist-regulated interaction of IKEPP and PDZK1 with the hIP (**Figure 9**), in addition to the role of these 2 closely related, but structurally and functionally distinct, NHERF members for prostacyclin regulated endothelial cell migration and *in vitro* angiogenesis. Under basal conditions, in the absence of agonist, both IKEPP and PDZK1 are constitutively associated in complexes with the hIP, where PDZ^{D1} of IKEPP and PDZ^{D3} PDZK1 are the preferential binding domains, respectively. While both IKEPP and PDZK1 [38] are phosphorylated in response to agonist (cicaprost)-activation of the hIP, an effect that is blocked by the selective IP antagonist RO1138452, their interaction with the hIP appears to be differentially modulated. More specifically, in response to agonist-activation of the hIP, there is an initial transient dissociation of PDZK1 from the hIP complex [38] while, in contrast to this, there is an initial increase in the interaction of IKEPP with the activated hIP (**Figure 6**). In the case of PDZK1, the agonist-regulated interaction involves direct hIP-induced cAMP-dependent PKA phosphorylation of PDZK1, where Ser^{505} within its C-terminal regulatory domain was identified as the specific phosphotarget [38]. On the other hand, inhibition of both PKA or PKC are necessary to impair the agonist-regulated interaction between IKEPP with the hIP suggesting that activation of the cAMP- and inositol phosphate-signalling cascades of the hIP are necessary to modulate its interaction with IKEPP [28, 30]. Furthermore, as stated, evidence of an interaction between the hIP and IKEPP endogenously expressed in vascular endothelial cells (1^{o} HUVECs) was confirmed through both co-immunoprecipitation and immunocytochemical approaches (**Figure 7C & 7D**, respectively) and that this interaction occurs constitutively, in the absence of agonist. While beyond the remit of the current study, it will be of interest to investigate the influence of cicaprost on the interaction and co-localization of the hIP and IKEPP within the vascular endothelium and, more specifically, whether the interaction is regulated in an agonist-dependent manner. Consistent with their functional expression in vascular endothelial cells, *si*RNA- targeted disruption of both PDZK1 [38] and IKEPP was found to specifically impair prostacyclin-induced endothelial cell migration and *in vitro* angiogenesis. Taken together, our findings establish a role for IKEPP in the vasculature where it regulates hIP-mediated endothelial migration and angiogenesis.

The discovery that the hIP interacts with both PDZK1 and IKEPP, NHERF proteins that show both over-lapping but also distinct (i) patterns of expression, (ii) interacting partners coupled with key (iii) structural and (iv) functional differences, reveals further insights into the factors regulating this complex 'I Prostanoid receptor'. Furthermore, detailed investigation of the functional interplay of the two NHERF members in the regulation of the hIP should lead to significant new insights into the role of this important receptor and of those PDZ adapter proteins within the vascular, renal, gastrointestinal and pulmonary systems where they and their key interacting partners are most abundantly expressed.

Acknowledgements:
This work was supported by Science Foundation of Ireland (Grant SFI:05/IN.1/B19).

REFERENCES

[1] P. Jemth, S. Gianni, PDZ domains: folding and binding, Biochemistry 46 (2007) 8701-8708.

[2] H.J. Lee, J.J. Zheng, PDZ domains and their binding partners: structure, specificity, and modification, Cell Commun Signal 8 (2010) 8.

[3] R. Tonikian, Y. Zhang, S.L. Sazinsky, B. Currell, J.H. Yeh, B. Reva, H.A. Held, B.A. Appleton, M. Evangelista, Y. Wu, X. Xin, A.C. Chan, S. Seshagiri, L.A. Lasky, C. Sander, C. Boone, G.D. Bader, S.S. Sidhu, A specificity map for the PDZ domain family, PLoS Biol 6 (2008) e239.

[4] G. Lamprecht, U. Seidler, The emerging role of PDZ adapter proteins for regulation of intestinal ion transport, Am J Physiol Gastrointest Liver Physiol 291 (2006) G766-777.

[5] W.R. Thelin, C.A. Hodson, S.L. Milgram, Beyond the brush border: NHERF4 blazes new NHERF turf, J Physiol 567 (2005) 13-19.

[6] O. Kocher, N. Comella, K. Tognazzi, L.F. Brown, Identification and partial characterization of PDZK1: a novel protein containing PDZ interaction domains, Lab Invest 78 (1998) 117-125.

[7] R.O. Scott, W.R. Thelin, S.L. Milgram, A novel PDZ protein regulates the activity of guanylyl cyclase C, the heat-stable enterotoxin receptor, J Biol Chem 277 (2002) 22934-22941.

[8] S.M. Gisler, I. Stagljar, M. Traebert, D. Bacic, J. Biber, H. Murer, Interaction of the type IIa Na/Pi cotransporter with PDZ proteins, J Biol Chem 276 (2001) 9206-9213.

[9] S.F. van de Graaf, J.G. Hoenderop, A.W. van der Kemp, S.M. Gisler, R.J. Bindels, Interaction of the epithelial Ca2+ channels TRPV5 and TRPV6 with the intestine- and kidney-enriched PDZ protein NHERF4, Pflugers Arch 452 (2006) 407-417.

[10] M.A. Lanaspa, H. Giral, S.Y. Breusegem, N. Halaihel, G. Baile, J. Catalan, J.A. Carrodeguas, N.P. Barry, M. Levi, V. Sorribas, Interaction of MAP17 with NHERF3/4 induces translocation of the renal Na/Pi IIa transporter to the trans-Golgi, Am J Physiol Renal Physiol 292 (2007) F230-242.

[11] N.C. Zachos, C. Hodson, O. Kovbasnjuk, X. Li, W.R. Thelin, B. Cha, S. Milgram, M. Donowitz, Elevated intracellular calcium stimulates NHE3 activity by an IKEPP (NHERF4) dependent mechanism, Cell Physiol Biochem 22 (2008) 693-704.

[12] T. Hegedus, T. Sessler, R. Scott, W. Thelin, E. Bakos, A. Varadi, K. Szabo, L. Homolya, S.L. Milgram, B. Sarkadi, C-terminal phosphorylation of MRP2 modulates its interaction with PDZ proteins, Biochem Biophys Res Commun 302 (2003) 454-461.

[13] C. Watanabe, Y. Kato, T. Sugiura, Y. Kubo, T. Wakayama, S. Iseki, A. Tsuji, PDZ adaptor protein PDZK2 stimulates transport activity of organic cation/carnitine transporter OCTN2 by modulating cell surface expression, Drug Metab Dispos 34 (2006) 1927-1934.

[14] G. Lamprecht, V. Gaco, J.R. Turner, D. Natour, M. Gregor, Regulation of the intestinal anion exchanger DRA (downregulated in adenoma), Ann N Y Acad Sci 1165 (2009) 261-266.

[15] S. Lissner, L. Nold, C.J. Hsieh, J.R. Turner, M. Gregor, L. Graeve, G. Lamprecht, Activity and PI3-kinase dependent trafficking of the intestinal anion exchanger downregulated in adenoma depend on its PDZ interaction and on lipid rafts, Am J Physiol Gastrointest Liver Physiol 299 (2010) G907-920.

[16] S. Narumiya, Y. Sugimoto, F. Ushikubi, Prostanoid receptors: structures, properties, and functions, Physiological reviews 79 (1999) 1193-1226.

[17] D.F. Woodward, R.L. Jones, S. Narumiya, International Union of Basic and Clinical Pharmacology. LXXXIII: classification of prostanoid receptors, updating 15 years of progress, Pharmacol Rev 63 (2011) 471-538.

[18] S. Narumiya, T. Furuyashiki, Fever, inflammation, pain and beyond: prostanoid receptor research during these 25 years, FASEB J 25 (2011) 813-818.

[19] J. Stitham, C. Midgett, K.A. Martin, J. Hwa, Prostacyclin: an inflammatory paradox, Front Pharmacol 2 (2011) 24.

[20] M.A. Tennis, M. Van Scoyk, L.E. Heasley, K. Vandervest, M. Weiser-Evans, S. Freeman, R.L. Keith, P. Simpson, R.A. Nemenoff, R.A. Winn, Prostacyclin inhibits non-small cell lung cancer growth by a frizzled 9-dependent pathway that is blocked by secreted frizzled-related protein 1, Neoplasia 12 (2010) 244-253.

[21] M.A. Tennis, M. Vanscoyk, R.L. Keith, R.A. Winn, The role of prostacyclin in lung cancer, Transl Res 155 (2010) 57-61.

[22] J. Kawabe, F. Ushikubi, N. Hasebe, Prostacyclin in vascular diseases. - Recent insights and future perspectives, Circ J 74 (2010) 836-843.

[23] J. Kawabe, K. Yuhki, M. Okada, T. Kanno, A. Yamauchi, N. Tashiro, T. Sasaki, S. Okumura, N. Nakagawa, Y. Aburakawa, N. Takehara, T. Fujino, N. Hasebe, S. Narumiya, F. Ushikubi, Prostaglandin I2 promotes recruitment of endothelial progenitor cells and limits vascular remodeling, Arterioscler Thromb Vasc Biol 30 (2010) 464-470.

[24] R. Nasrallah, J. Clark, R.L. Hebert, Prostaglandins in the kidney: developments since Y2K, Clin Sci (Lond) 113 (2007) 297-311.

[25] R. Nasrallah, R.L. Hebert, Prostacyclin signaling in the kidney: implications for health and disease, Am J Physiol Renal Physiol 289 (2005) F235-246.

[26] R.N. Channick, R. Voswinckel, L.J. Rubin, Inhaled treprostinil: a therapeutic review, Drug Des Devel Ther 6 (2012) 19-28.

[27] M. Gomberg-Maitland, H. Olschewski, Prostacyclin therapies for the treatment of pulmonary arterial hypertension, Eur Respir J 31 (2008) 891-901.

[28] O.A. Lawler, S.M. Miggin, B.T. Kinsella, Protein kinase A-mediated phosphorylation of serine 357 of the mouse prostacyclin receptor regulates its coupling to G(s)-, to G(i)-, and to G(q)-coupled effector signaling, J Biol Chem 276 (2001) 33596-33607.

[29] C. Midgett, J. Stitham, K.A. Martin, J. Hwa, Prostacyclin receptor regulation--from transcription to trafficking, Curr Mol Med 11 (2011) 517-528.

[30] S.M. Miggin, B.T. Kinsella, Investigation of the mechanisms of G protein: effector coupling by the human and mouse prostacyclin receptors. Identification of critical species-dependent differences, J Biol Chem 277 (2002) 27053-27064.

[31] J.S. Hayes, O.A. Lawler, M.T. Walsh, B.T. Kinsella, The prostacyclin receptor is isoprenylated. Isoprenylation is required for efficient receptor-effector coupling, J Biol Chem 274 (1999) 23707-23718.

[32] S.M. Miggin, O.A. Lawler, B.T. Kinsella, Palmitoylation of the human prostacyclin receptor. Functional implications of palmitoylation and isoprenylation, J Biol Chem 278 (2003) 6947-6958.

[33] H.M. Reid, E.P. Mulvaney, E.C. Turner, B.T. Kinsella, Interaction of the human prostacyclin receptor with Rab11: characterization of a novel Rab11 binding domain within alpha-helix 8 that is regulated by palmitoylation, J Biol Chem 285 (2010) 18709-18726.

[34] K. Wikstrom, H.M. Reid, M. Hill, K.A. English, M.B. O'Keeffe, C.C. Kimbembe, B.T. Kinsella, Recycling of the human prostacyclin receptor is regulated through a direct interaction with Rab11a GTPase, Cellular signalling 20 (2008) 2332-2346.

[35] J. Bockaert, L. Fagni, A. Dumuis, P. Marin, GPCR interacting proteins (GIP), Pharmacol Ther 103 (2004) 203-221.

[36] J. Bockaert, G. Roussignol, C. Becamel, S. Gavarini, L. Joubert, A. Dumuis, L. Fagni, P. Marin, GPCR-interacting proteins (GIPs): nature and functions, Biochem Soc Trans 32 (2004) 851-855.

[37] J. Bockaert, P. Marin, A. Dumuis, L. Fagni, The 'magic tail' of G protein-coupled receptors: an anchorage for functional protein networks, FEBS Lett 546 (2003) 65-72.

[38] E.C. Turner, E.P. Mulvaney, H.M. Reid, B.T. Kinsella, Interaction of the human prostacyclin receptor with the PDZ adapter protein PDZK1: role in endothelial cell migration and angiogenesis, Mol Biol Cell 22 (2011) 2664-2679.

[39] M. Abramovitz, Y. Boie, T. Nguyen, T.H. Rushmore, M.A. Bayne, K.M. Metters, D.M. Slipetz, R. Grygorczyk, Cloning and expression of a cDNA for the human prostanoid FP receptor, J Biol Chem 269 (1994) 2632-2636.

[40] H.A. Bilson, D.L. Mitchell, B. Ashby, Human prostaglandin EP3 receptor isoforms show different agonist-induced internalization patterns, FEBS Lett 572 (2004) 271-275.

[41] H.M. Reid, K. Wikstrom, D.J. Kavanagh, E.P. Mulvaney, B.T. Kinsella, Interaction of angio-associated migratory cell protein with the TPalpha and TPbeta isoforms of the human thromboxane A(2) receptor, Cellular signalling 23 (2011) 700-717.

[42] D.A. Doyle, A. Lee, J. Lewis, E. Kim, M. Sheng, R. MacKinnon, Crystal structures of a complexed and peptide-free membrane protein-binding domain: molecular basis of peptide recognition by PDZ, Cell 85 (1996) 1067-1076.

[43] R.D. Finn, J. Mistry, J. Tate, P. Coggill, A. Heger, J.E. Pollington, O.L. Gavin, P. Gunasekaran, G. Ceric, K. Forslund, L. Holm, E.L. Sonnhammer, S.R. Eddy, A. Bateman, The Pfam protein families database, Nucleic Acids Res 38 (2010) D211-222.

[44] M.B. O'Keeffe, H.M. Reid, B.T. Kinsella, Agonist-dependent internalization and trafficking of the human prostacyclin receptor: a direct role for Rab5a GTPase, Biochim Biophys Acta 1783 (2008) 1914-1928.

[45] C.M. Gorman, D. Gies, G. McCray, Transient production of proteins using an adenovirus transformed cell line, DNA Protein Eng. Tech. 2 (1990) 3-10.
[46] J.E. Suggs, M.C. Madden, M. Friedman, C.J. Edgell, Prostacyclin expression by a continuous human cell line derived from vascular endothelium, Blood 68 (1986) 825-829.
[47] E.C. Turner, B.T. Kinsella, Estrogen increases expression of the human prostacyclin receptor within the vasculature through an ERalpha-dependent mechanism, J Mol Biol 396 (2010) 473-486.
[48] J.H. Han, S. Batey, A.A. Nickson, S.A. Teichmann, J. Clarke, The folding and evolution of multidomain proteins, Nat Rev Mol Cell Biol 8 (2007) 319-330.
[49] O. Kocher, M. Krieger, Role of the adaptor protein PDZK1 in controlling the HDL receptor SR-BI, Curr Opin Lipidol 20 (2009) 236-241.
[50] P.D. Donnellan, C.C. Kimbembe, H.M. Reid, B.T. Kinsella, Identification of a novel endoplasmic reticulum export motif within the eighth alpha-helical domain (alpha-H8) of the human prostacyclin receptor, Biochim Biophys Acta 1808 (2011) 1202-1218.
[51] T. Nakamura, N. Shibata, T. Nishimoto-Shibata, D. Feng, M. Ikemoto, K. Motojima, O.N. Iso, K. Tsukamoto, M. Tsujimoto, H. Arai, Regulation of SR-BI protein levels by phosphorylation of its associated protein, PDZK1, Proc Natl Acad Sci U S A 102 (2005) 13404-13409.
[52] J.W. Voltz, M. Brush, S. Sikes, D. Steplock, E.J. Weinman, S. Shenolikar, Phosphorylation of PDZ1 domain attenuates NHERF-1 binding to cellular targets, J Biol Chem 282 (2007) 33879-33887.
[53] M. Komhoff, B. Lesener, K. Nakao, H.W. Seyberth, R.M. Nusing, Localization of the prostacyclin receptor in human kidney, Kidney Int 54 (1998) 1899-1908.
[54] R. Nasrallah, R.M. Nusing, R.L. Hebert, Localization of IP in rabbit kidney and functional role of the PGI(2)/IP system in cortical collecting duct, Am J Physiol Renal Physiol 283 (2002) F689-698.
[55] M. Donowitz, B. Cha, N.C. Zachos, C.L. Brett, A. Sharma, C.M. Tse, X. Li, NHERF family and NHE3 regulation, J Physiol 567 (2005) 3-11.
[56] Y. Kato, Y. Sai, K. Yoshida, C. Watanabe, T. Hirata, A. Tsuji, PDZK1 directly regulates the function of organic cation/carnitine transporter OCTN2, Mol Pharmacol 67 (2005) 734-743.
[57] Y. Kato, K. Yoshida, C. Watanabe, Y. Sai, A. Tsuji, Screening of the interaction between xenobiotic transporters and PDZ proteins, Pharm Res 21 (2004) 1886-1894.
[58] E.J. Weinman, D. Steplock, Y. Zhang, R. Biswas, R.J. Bloch, S. Shenolikar, Cooperativity between the phosphorylation of Thr95 and Ser77 of NHERF-1 in the hormonal regulation of renal phosphate transport, J Biol Chem 285 (2010) 25134-25138.
[59] J.A. Ardura, P.A. Friedman, Regulation of G Protein-Coupled Receptor Function by Na+/H+ Exchange Regulatory Factors, Pharmacol Rev 63 (2011) 882-900.
[60] T. Fujino, N. Nakagawa, K. Yuhki, A. Hara, T. Yamada, K. Takayama, S. Kuriyama, Y. Hosoki, O. Takahata, T. Taniguchi, J. Fukuzawa, N. Hasebe, K. Kikuchi, S. Narumiya, F. Ushikubi, Decreased susceptibility to renovascular hypertension in mice lacking the prostaglandin I2 receptor IP, J Clin Invest 114 (2004) 805-812.
[61] V.D. Garovic, S.C. Textor, Renovascular hypertension and ischemic nephropathy, Circulation 112 (2005) 1362-1374.
[62] K. Yuhki, F. Kojima, H. Kashiwagi, J. Kawabe, T. Fujino, S. Narumiya, F. Ushikubi, Roles of prostanoids in the pathogenesis of cardiovascular diseases: Novel insights from knockout mouse studies, Pharmacol Ther 129 (2011) 195-205.

FIGURE LEGENDS

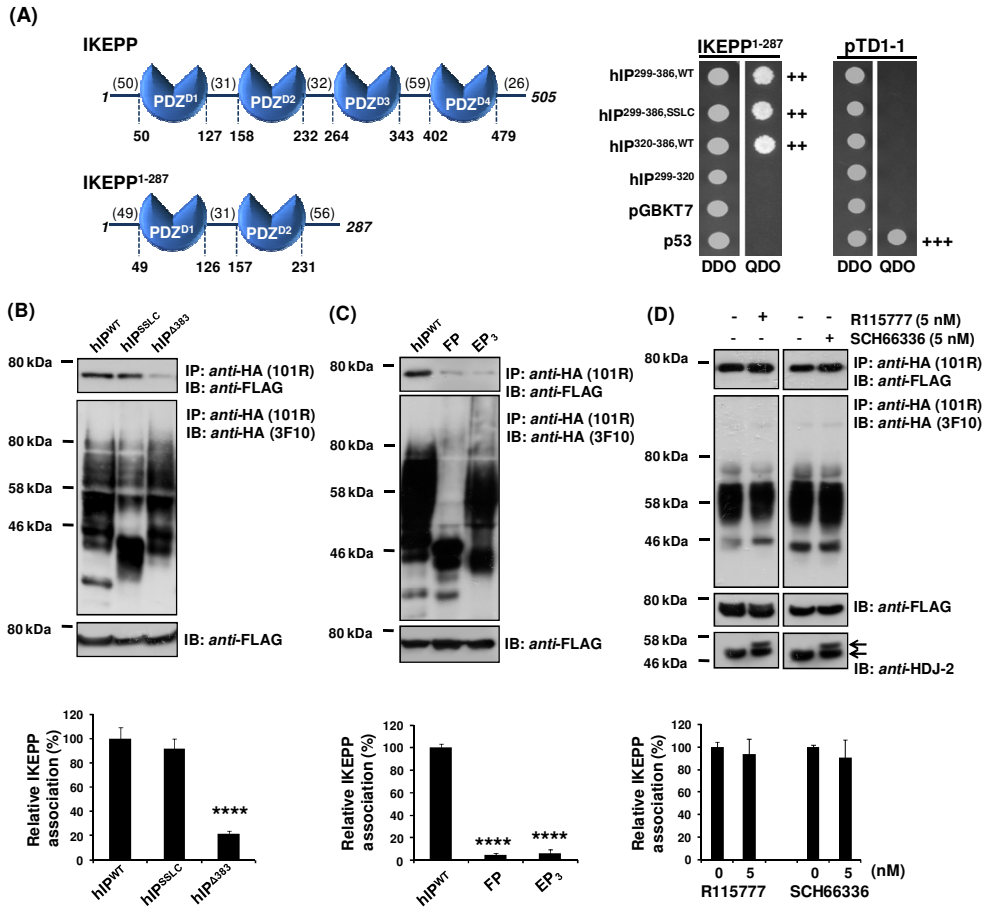

Figure 1. Interaction of IKEPP with the Human Prostacyclin Receptor

Panel A: Schematic of the full length IKEPP, encoding 4 PDZ domains, and IKEPP$^{1\text{-}287}$, encoding amino acids 1-287, corresponding to PDZ domains 1 and 2 only and which was originally identified as the hIP interactant. *S.c* Y187 (pACT2.IKEPP$^{1\text{-}287}$) and, as a control, *S.c.* Y187 (pTDI-I), encoding SV-40 large T-antigen, prey strains were mated with *S.c.* AH109 (pGBKT7.hIP) bait strains encoding the listed hIP sub-fragments and as controls, p53 or vector (pGBKT7) alone. Diploids were selected on DDO medium, whereas interactants were selected on QDO medium. Data; n ≥ 3. **Panels B - C:** HEK.hIP^{WT}, HEK.hIP^{SSLC} and HEK.hIP$^{\Delta 383}$ cells transiently transfected with plasmid (pCMVTag2C) encoding FLAG-tagged IKEPP (**Panel B**) or HEK 293 cells transiently co-transfected FLAG-tagged IKEPP, HA-tagged FP or HA-tagged EP_3 (**Panel C**) were immunoprecipitated with *anti*-HA 101R antibody. **Panel D:** HEK.hIP^{WT} cells, transiently transfected with FLAG-tagged IKEPP, were pre-incubated with the farnesyl transferase inhibitors R115777 (5 nM), SCH66336 (5 nM) or, as a control, with drug vehicle for 24 hr prior to immunoprecipitation with *anti*-HA 101R antibody. Immunoprecipitates (IP) in **B – D** were immunoblotted (IB) using either *anti*-FLAG or *anti*-HA (3F10) antisera to detect FLAG-tagged IKEPP or HA-tagged hIP, FP or EP_3 receptors (**Panel A –D**; upper and middle panels, respectively). Uniform expression of FLAG-tagged IKEPP was verified by immunoblot analysis of whole cell lysates (50 µg/lane) with *anti*-FLAG antibody (lower panels). The efficacy of R115777 or SCH66336 to inhibit general protein farnesylation was validated by immunoblot analysis of whole cell lysates (50 µg/lane) for the farnesylated (~ 45-46 kDa) and non-farnesylated (49 kDa) species of the molecular chaperone HDJ-2, as indicated by the arrows (**Panel D**, *anti*-HDJ-2; lower panels). The bar chart shows mean relative levels of IKEPP associated with the *anti*-HA 101R immunoprecipitates (relative protein, % ± SEM, $n = 3$). Asterisks indicate that levels of IKEPP found in the *anti*-HA immunoprecipitates were significantly reduced compared to that from HEK.hIP cells, encoding the wild type HA:hIP, where **** indicates $p < 0.0001$, for post-hoc Dunnett's multiple comparison *t*-test analysis.

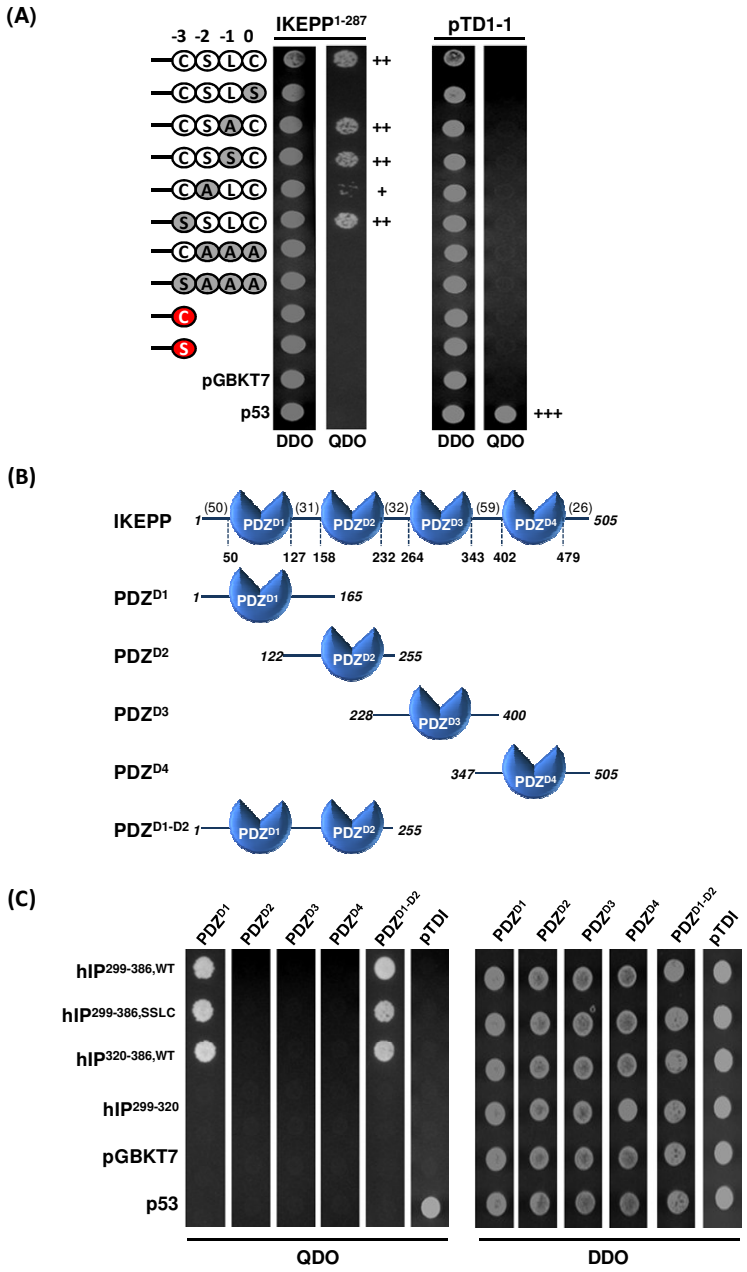

Figure 2: Characterization of the PDZ Ligand within the C-tail Domain of the hIP and Identification of the PDZ Domains within IKEPP Involved in the Interaction with the hIP

Panel A: *S.c* Y187 (pACT2.IKEPP$^{1-287}$) or, as a control, *S.c* Y187 (pTDI-I) prey strains were mated with the *S.c* AH109 (pGBKT7.hIP$^{299-386}$) bait strains (encoding either wild type (WT) or variants of hIP$^{299-386}$, where the -C^{383}SLC^{386} carboxyl-terminal residues corresponding to the positions $(P)_0$, P_{-1}, P_{-2}, and P_{-3} of its PDZ ligand were mutated as indicated) or, as controls, p53 or the vector (pGBKT7) alone. **Panel B:** Schematic showing full length IKEPP and the sub-fragments, encoding its individual PDZ domains PDZ^{D1} – PDZ^{D4}, generated for this study. **Panel C:** *S.c* Y187 (pACT2) expressing the listed IKEPP sub-fragments encoding individual or paired PDZ domains, as indicated, were mated with *S.c.* AH109 (pGBKT7) encoding the listed hIP subfragments and, as controls, p53 or the vector pGBKT7 alone. Diploids were selected on DDO medium, whereas interactants were selected on QDO medium. Data; $n \geq 3$.

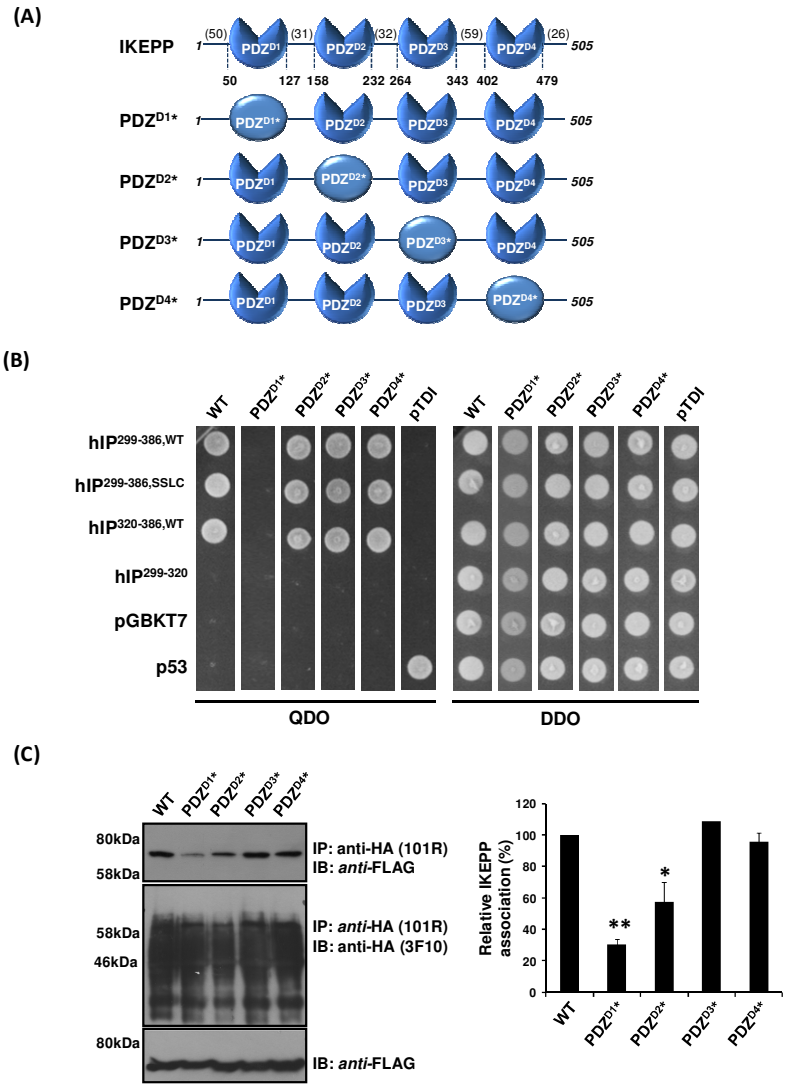

Figure 3: Identification of the PDZ Domains within IKEPP Involved in the Interaction with the hIP
Panel A: Schematic of full length IKEPP with its 4 PDZ domains whereby the 'GLGF motif' mutated within each of the individual PDZ^{D1} – PDZ^{D4} domains are indicated by an asterisks (*). **Panel B:** S.c. Y187 (pACT2.IKEPP) prey strains, encoding the full length IKEPP where the 'GLGF motif' in each of the PDZ^{D1} – PDZ^{D4} domains are mutated (*; **Panel B**), as indicated, were mated with *S.c.* AH109 (pGBKT7) encoding the listed hIP subfragments and, as controls, p53 or the vector pGBKT7 alone. Diploids were selected on DDO medium, whereas interactants were selected on QDO medium. Data; n ≥ 3. **Panel C:** HEK.hIP cells were transiently transfected with pCMVTag2C plasmids encoding FLAG-tagged forms of IKEPP, IKEPP^{PDZD1*}, IKEPP^{PDZD2*}, IKEPP^{PDZD3*} and IKEPP^{PDZD4*}. After 48 hr, HA-tagged hIP was immunoprecipitated with *anti*-HA 101R antibody and immunoprecipitates (IP) were immunoblotted (IB) with *anti*-FLAG-IKEPP (upper panel) or *anti*-HA 3F10 (middle panel) antisera. Uniform expression of the FLAG-tagged IKEPP proteins was verified by immunoblot analysis of whole cell lysates (50 µg/lane) with *anti*-FLAG antibody (lower panel). The bar chart shows mean relative levels of the wild type and mutated forms of IKEPP associated with the *anti*-HA 101R immunoprecipitates (relative protein, % ± SEM, $n = 3$), where levels of the wild-type IKEPP are expressed as 100 %. The asterisks indicate where mutation of the GLGF sequence within the individual PDZ domains of IKEPP resulted in significant reductions in levels of IKEPP found in *anti*-HA:hIP precipitates, where ** and * indicate $p < 0.01$ and $p < 0.05$, respectively, for post-hoc Dunnett's multiple comparison *t*-test analysis.

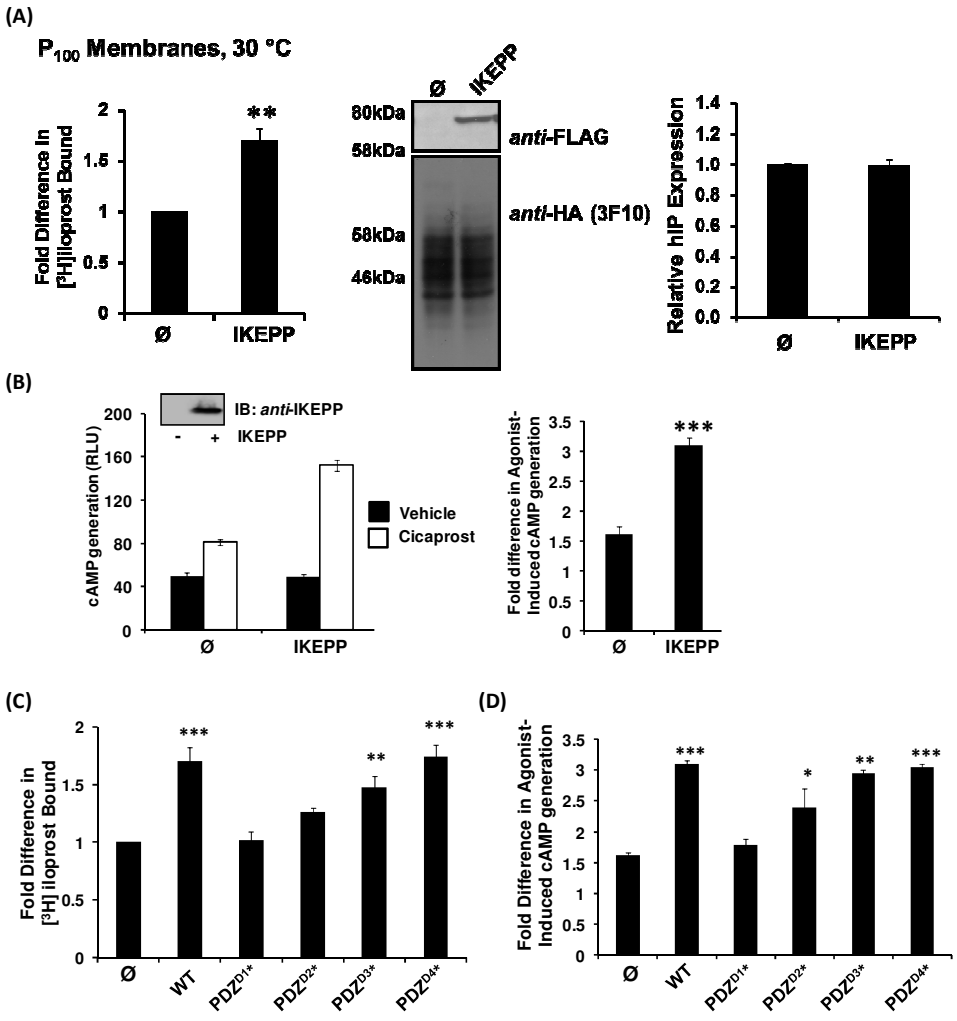

Figure 4: Effect of IKEPP on the Expression and Signalling of the hIP

Panels A & C: HEK.hIP^{WT} cells were transiently transfected with pCMVTag2C plasmids encoding FLAG-tagged forms of IKEPP, IKEPP^{PDZD1*}, IKEPP^{PDZD2*}, IKEPP^{PDZD3*} or IKEPP^{PDZD4*} or, as a control, with the vector alone (Ø). Radioligand binding analysis was performed 72 hr post-transfection in the presence of 4 nM [^{3}H]iloprost for 60 min using crude membrane (P_{100}) fractions. Data are presented as fold increases in [^{3}H]iloprost bound where levels in the presence of empty vector (Ø) are expressed as 1. Expression of IKEPP and the hIP was confirmed by immunoblot analysis with *anti*-FLAG (upper panel) and *anti*-HA 3F10 (lower panel) antisera (**Panel A**). The bar chart shows mean relative levels of the HA-tagged hIP expression in the presence of empty vector (Ø) or IKEPP (Mean ± SEM, $n = 3$), where levels of the hIP in the presence of vector alone are expressed as 1. **Panel B & D:** HEK293 cells were transiently co-transfected with pHM6:hIP, pADVA, pCRE-LUC and pRL-TK in the presence of vector encoding FLAG-tagged forms of IKEPP, IKEPP^{PDZD1*}, IKEPP^{PDZD2*}, IKEPP^{PDZD3*}, or IKEPP^{PDZD4*} or, as a control, with the vector alone (Ø). Cells were incubated either with vehicle or cicaprost (1 µM; 3 hr) prior to determination of cAMP generation, where data are represented as mean cAMP generation (RLU; **Panel B**, left panel) or fold inductions in agonist-induced cAMP accumulation (**Panel B**, right panel & **Panel D**). Transfection efficiency was confirmed through immunoblot analysis of the whole cell lysates (35 µg/lane) with *anti*-IKEPP antibody (**Panel B**, inset). The asterisks indicate significant increases in radioligand binding or cAMP generation in the presence of IKEPP, or its mutated variants, compared to that in the presence of the vector (Ø) alone, where ***, **, and * indicate $p < 0.001$, $p < 0.01$ and $p < 0.05$, respectively, for post-hoc Dunnett's multiple comparison *t*-test analysis.

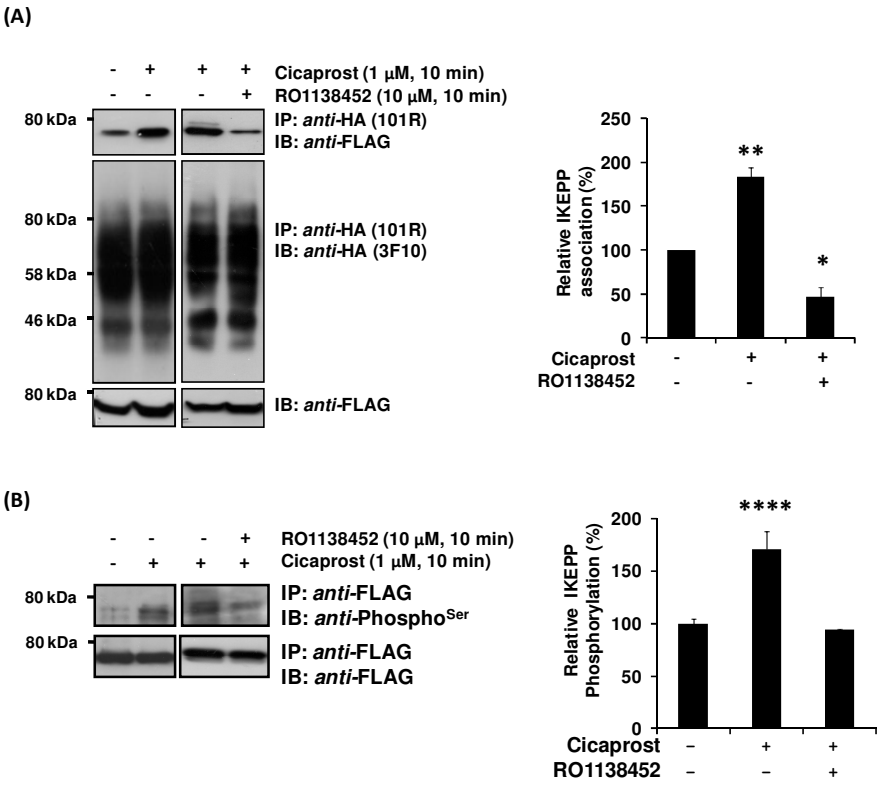

Figure 5: Effect of Agonist-activation of the hIP on the Interaction with IKEPP.
Panels A & B: HEK.hIP cells, transiently transfected with plasmid encoding FLAG-tagged IKEPP, were pre-incubated with vehicle or RO1138452 (10 μM; 10 min), followed by stimulation for 10 min with cicaprost (1 μM) or drug vehicle, as indicated, prior to immunoprecipitation with *anti*-HA 101R (**Panel A**) or *anti*-FLAG (**Panel B**) antibodies. Immunoprecipitates (IP) were immunoblotted (IB) with *anti*-FLAG (**Panel A**, upper panel; **Panel B**, lower panel), *anti*-HA 3F10 (**Panel A**, middle panel) or with *anti*-Phospho^{Ser} (**Panel B**, upper panel) antisera. Uniform expression of the FLAG-tagged IKEPP proteins was verified by immunoblot analysis of whole cell lysates (50 μg/lane) with *anti*-FLAG antibody (**Panel A**, lower panel). The bar charts show mean relative levels of FLAG-tagged IKEPP present in *anti*-HA 101R immunoprecipitates (**Panel A**; relative protein, % ± SEM, $n = 3$) or mean relative levels of the phosphoserine associated with the *anti*-FLAG immunoprecipitates (**Panel B**; relative protein, % ± SEM, $n = 3$) where levels in the absence of cicaprost or RO113852 are expressed as 100 %. Asterisks indicate a significant change in levels of IKEPP present in *anti*-HA immunoprecipitates or level of IKEPP phosphorylation compared to basal conditions where ****, ** and * indicates $p < 0.0001$, $p < 0.01$ and $p < 0.05$, respectively, for post-hoc Dunnett's multiple comparison *t*-test analysis.

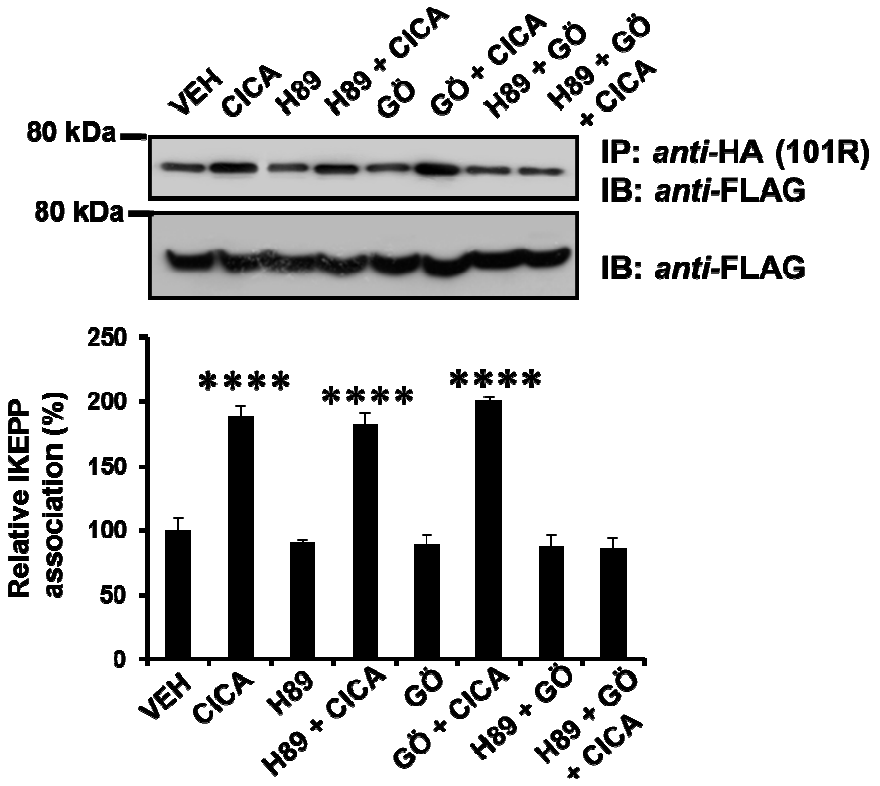

Figure 6: Involvement of PKA and PKC in the Interaction between IKEPP and the hIP
HEK.hIP cells, transiently transfected with plasmid encoding FLAG-tagged IKEPP, were pre-incubated with vehicle, H-89 (10 µM) or Gö6983 (1 µM; Gö), either alone or in combination for 10 min, prior to stimulation for 10 min with vehicle or cicaprost (1 µM; CICA). The hIP was immunoprecipitated with *anti*-HA 101R and immunoprecipitates (IP) were immunoblotted (IB) with *anti*-FLAG-IKEPP (upper panel) or *anti*-HA (3F10) antisera. Uniform expression of the FLAG-tagged IKEPP protein was verified by immunoblot analysis of whole cell lysates (50 µg/lane) with *anti*-FLAG antibody (lower panel). The bar chart shows mean relative levels of the IKEPP associated with the *anti*-HA 101R immunoprecipitates (relative protein, % ± SEM, $n = 3$) where levels in the absence of agonist are expressed as 100 %. The asterisks indicate that the levels of IKEPP found in *anti*-HA precipitates from cicaprost treated cells were significantly increased compared to basal conditions where **** indicates $p < 0.0001$.

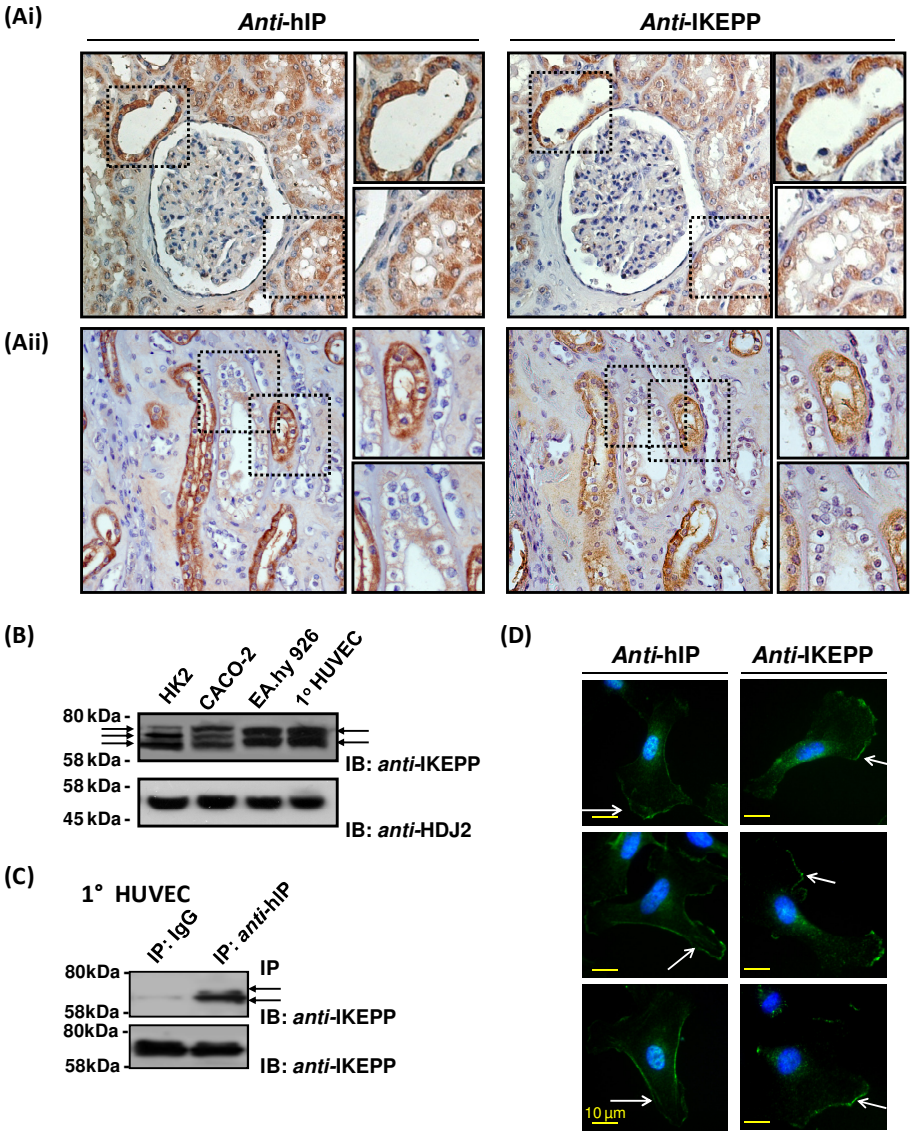

Figure 7: Expression of IKEPP and hIP

Panel A: Consecutive formalin-fixed, paraffin-embedded normal kidney sections were immunolabelled with *anti*-hIP and *anti*-IKEPP antibodies prior to immunodetection using Vectastain Universal Elite ABC kit. Images were captured at 20x magnification using a Zeiss microscope and Axiovision software. The upper panels (**Panel Ai**) represent the renal cortex, where the insets represent 2-fold magnifications of the indicated boxed regions corresponding to the distal (upper inset) and proximal (lower inset) tubules, respectively. The lower panels (**Panel Aii**) represent the renal medulla regions where the insets represent 2-fold magnifications of the indicated boxed regions. **Panel B:** Whole cell lysates (50 µg per lane) from human epithelial HK2, intestinal Caco-2, human endothelial EA.hy926 cells and 1° HUVECs (25 µg) were resolved by SDS-PAGE and immunoblotted with *anti*-IKEPP and *anti*-HDJ2, where arrows indicate the presence of multiple IKEPP isoforms. **Panel C:** 1° HUVECs were immunoprecipitated with *anti*-hIP antibody or, as a control, with pre-immune IgG. Immunoprecipitates (IP) were immunoblotted (IB) with *anti*-IKEPP (upper panel). Expression of endogenous IKEPP was verified by immunoblot analysis of whole cell lysates (50 µg/lane) with *anti*-IKEPP antibody (lower panel). **Panel D:** 1° HUVECs were immunolabelled with *anti*-hIP or *anti*-IKEPP antibodies prior to detection with AlexaFluor488 goat *anti*-rabbit secondary antibody. Images were captured at 63x magnification using a Zeiss microscope and Axiovision software.

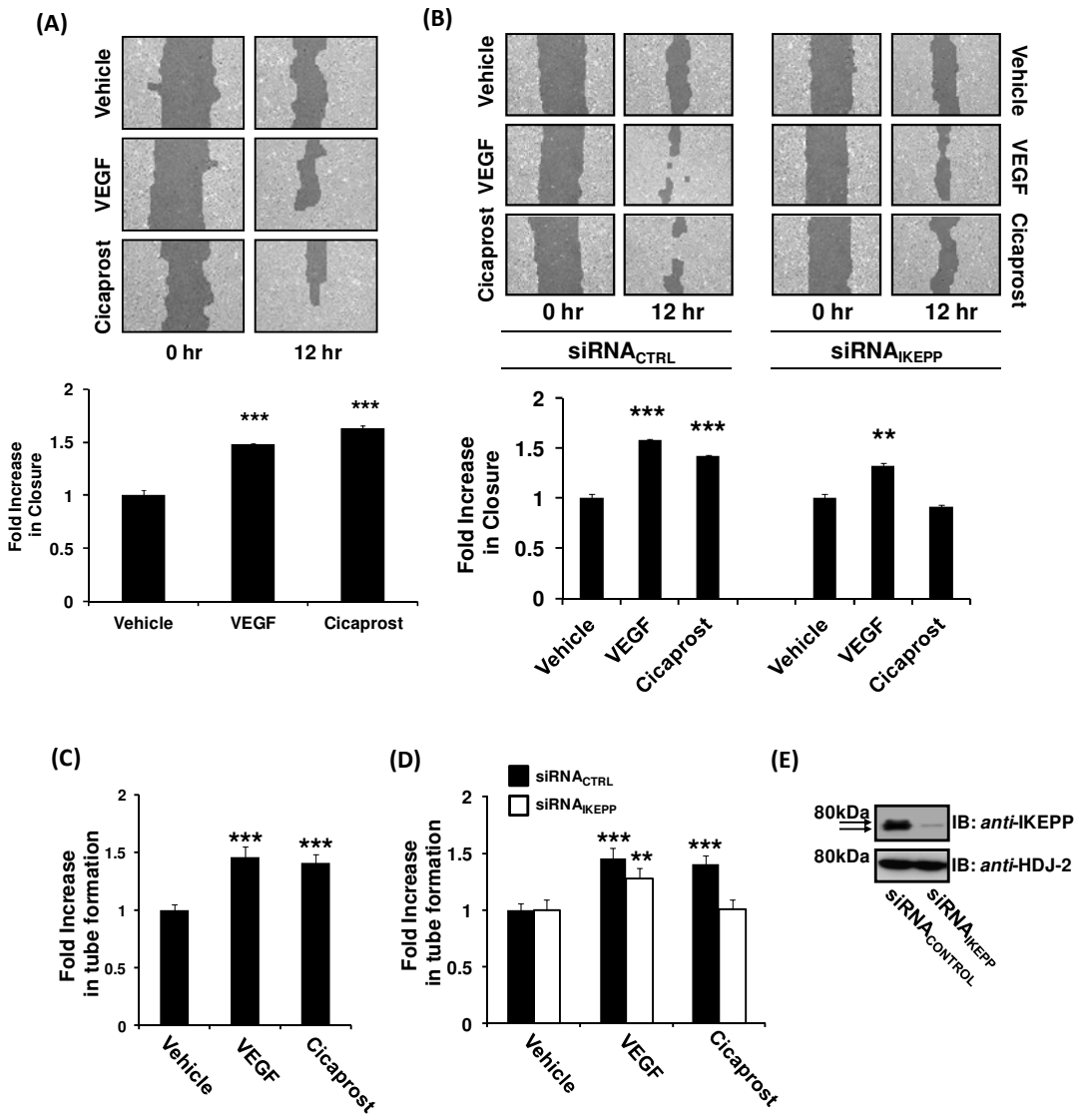

Figure 8: Effect of IKEPP on hIP Agonist-induced Migration and Tube Formation in 1° HUVECs
Migration (**Panel A & B**) and tube formation (**Panels C & D**) by primary (1°) HUVECs were analyzed at 0 hr and 12 hr in following incubation with drug vehicle, VEGF or cicaprost, as indicated, in either non-transfected cells (**Panels A & C**) or in cells transfected with *si*RNA$_{CTRL}$ or *si*RNA$_{IKEPP}$ (**Panels B & D**), where immunoblot analysis confirmed specific disruption of IKEPP expression (**Panel E**). Bar charts represent mean fold increases (± SEM; n = 3) in either wound closure or tube length in the presence of vehicle, VEGF or cicaprost, as indicated, at 12 hr. The asterisks indicate either significant agonist-induced increases in migration (**Panels A & B**) or significant agonist-induced increases in tube length (**Panels C & D**) in comparison to vehicle-treated cells where **, and *** indicate $p < 0.01$, and $p < 0.001$, respectively, for post hoc Dunnett's multiple comparison t-test analysis.

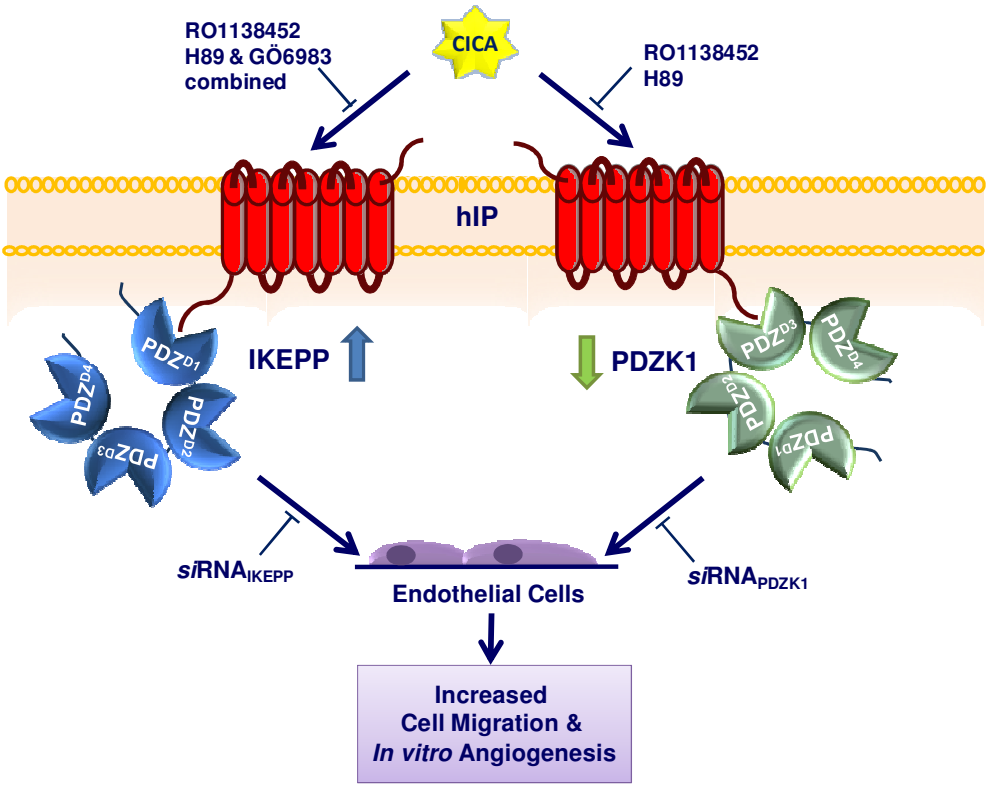

Figure 9: Model of the Interaction between the hIP and IKEPP
In the absence of agonist, both IKEPP and PDZK1 are constitutively associated in a complex with the hIP where these interactions are largely dependent on PDZ domain 1 (PDZ^{D1}), and to a lesser extent PDZ^{D2}, of IKEPP, and PDZ^{D3}, and to a lesser extent PDZ^{D1} and PDZ^{D4}, of PDZK1 [38], respectively. Upon cicaprost stimulation (10 min; CICA), the association of IKEPP and PDZK1 with the hIP is differentially modulated. More specifically, the association of IKEPP with the hIP is enhanced in response to receptor activation, an effect that is abrogated by the selective IP antagonist RO1138452 and the combined activity of the PKA and PKC inhibitors, H-89 and Gö6983, respectively. On the other hand, in response to cicaprost (10 min) stimulation, there is a transient disassociation of PDKZ1 from the hIP complex and this occurs due to hIP-induced PKA phosphorylation of Ser^{505} within the C-terminal regulatory domain of IKEPP [38]. Herein, and previously [38], it was established that cicaprost stimulation promotes endothelial cell migration and tube formation, a measure of *in vitro* angiogenesis, and that these effects are impaired by the selective IP antagonist RO1138452. siRNA-mediated targeted disruption of both IKEPP and PDZK1 [38] expression specifically impairs cicaprost-induced endothelial cell migration and *in vitro* angiogenesis.

SUPPLEMENTAL DATA:

SUPPLEMENTAL TABLE 1. SITE SPECIFIC MUTATIONS, AND PRIMERS USED, TO DISRUPT THE 'GLGF MOTIF' WITHIN THE HYDROPHOBIC BINDING POCKET OF PDZ^{D1-D4} OF IKEPP.

WILD TYPE 'GLGF MOTIF'	MUTATED 'GLGF MOTIF'	RECOMBINANT PLASMID GENERATED	OLIGONUCLEOTIDE PRIMER USED IN SITE-DIRECTED MUTAGENESIS†
PDZ^{D1}: S$F^{60}G^{61}$F	S***R***^{60}***E***^{61}F	pACT2: IKEPP^{PDZ1*}/ pCMVTag2C:IKEPP^{PDZ1*}/ pACT2: IKEPP$^{1-287\ PDZ1*}$	5'CAAAGAGGAGGGCAAGAGT***CG***TG ***AG***TTCCACCTGCAGCAGGAGC-3'
PDZ^{D2}: G$F^{167}G^{168}$F	G***R***^{167}***E***^{168}F	pACT2: IKEPP^{PDZ2*}/ pCMVTag2C:IKEPP^{PDZ2*}/ pACT2: IKEPP$^{1-287\ PDZ2*}$	5'CATAGTGAAAGATGAGGGTGGT***CG*** TG***AG***TTCAGTGTCACCCATGGCAAT C-3'
PDZ^{D3}: $G^{271}FR^{273}F^{274}$	***K***^{271}F***R***^{273}***E***^{274}	pACT2: IKEPP^{PDZ3*}/ pCMVTag2C:IKEPP^{PDZ3*}	5'GAGAAAGGGCCCCAG***AAA***TTT***C***GG T***C***CCTGCTCCGGGAGGAAAAG-3'
PDZ^{D4}: $SYG^{413}F^{414}$	SY***R***^{413}***E***^{414}	pACT2: IKEPP^{PDZ4*}/ pCMVTag2C:IKEPP^{PDZ4*}	5'GGGCCTGGTGGCAGCTAT***C***GC***GAG*** CGACTCAGTTGTGT-3'

† Sequences given correspond to those of the sense primer only where the identity of the mutator codon(s) is in boldface italics and antisense primer sequences are inferred.

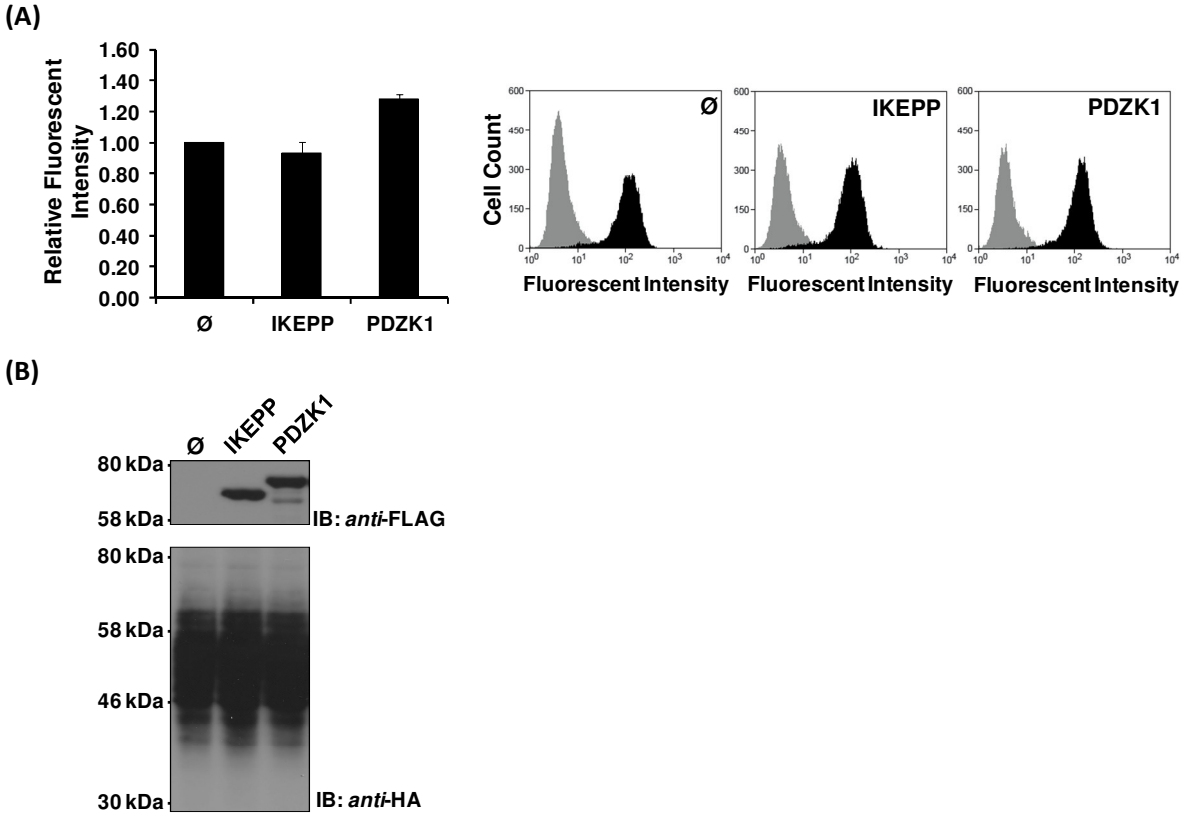

Supplemental Figure 1. Effect of IKEPP on the expression of the hIP.
Panels A & B: HEK.hIP cells were transiently transfected with pCMVTag2C plasmid encoding FLAG-tagged IKEPP, PDZK1 or, as control, with vector (Ø) alone. Expression of the HA-tagged hIP at the cell surface was examined through flow cytometric analysis, using *anti*-HA (101R) and AlexaFluor488 goat *anti*-mouse antibodies (**Panel A**). In parallel, cells were immunolabelled with normal IgG to control for background fluorescence. The bar charts represent relative fluorescent intensity where levels in control-transfected cells are assigned a value of 1. Representative flow cytometry histograms show the cell surface expression of the HA-tagged hIP (black) compared to background (grey), where the horizontal axis show fluorescence intensity and the vertical axis represents cell count. Immunoblot (IB) analysis confirmed expression of FLAG-tagged IKEPP and PDZK1 (**Panel B**, *anti*-FLAG) and uniform expression of the HA-tagged hIP (**Panel B**, *anti*-HA).

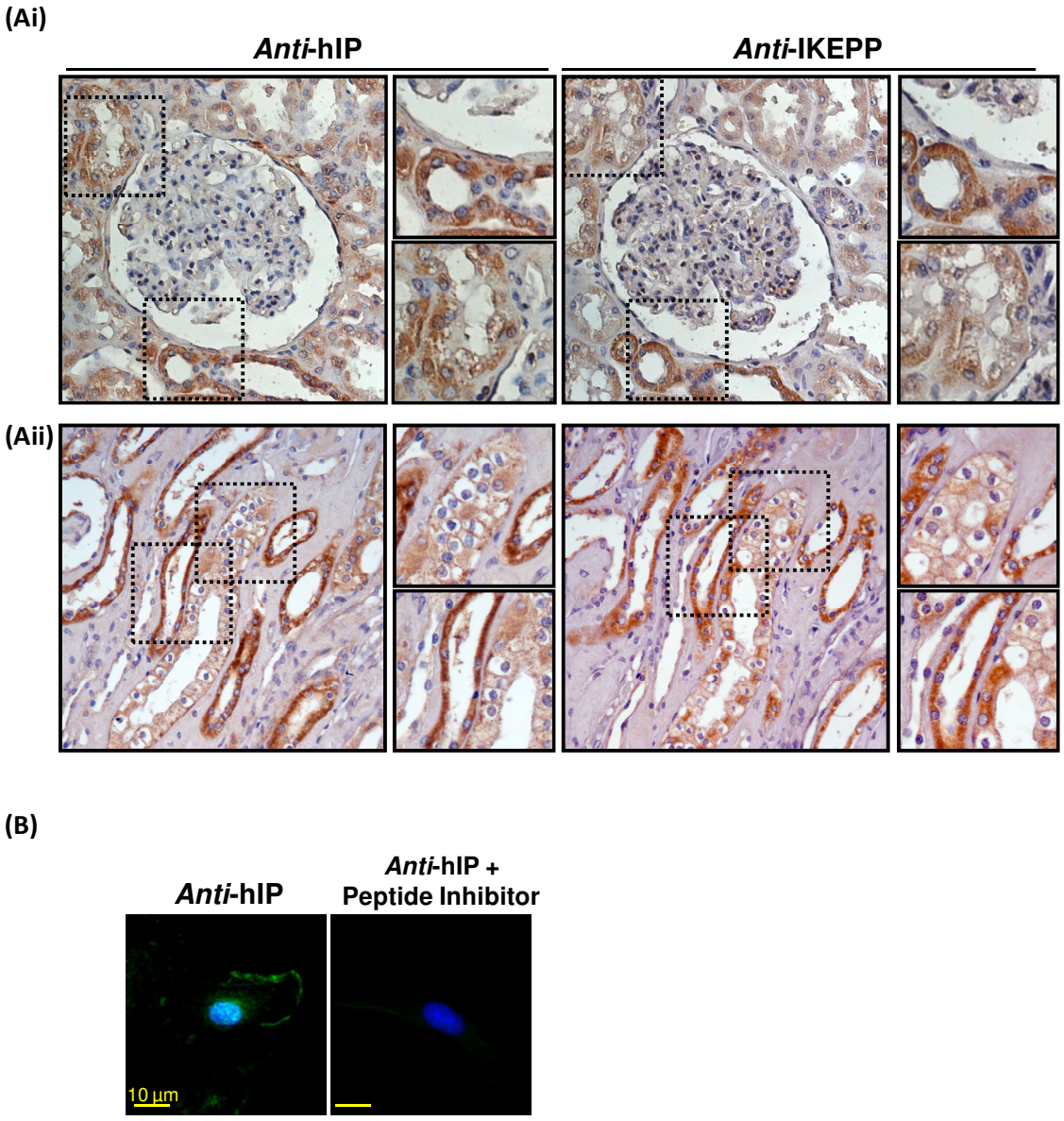

Supplemental Figure 2. Expression of IKEPP and hIP in the Human Kidney
Panel A: Consecutive formalin-fixed, paraffin-embedded normal kidney sections were immunolabelled with *anti*-hIP and *anti*-IKEPP antibodies prior to immunodetection using Vectastain Universal Elite ABC kit. Images were captured at 20x magnification using a Zeiss microscope and Axiovision software. The upper panels (**Panel 2Ai**) represent the renal cortex, where the insets represent 2-fold magnifications of the indicated boxed regions corresponding to the distal (upper inset) and proximal (lower inset) tubules, respectively. The lower panels (**Panel 2Aii**) represent the renal medulla regions where the insets represent 2-fold magnifications of the indicated boxed regions. **Panel B:** 1° HUVECs were immunolabelled with *anti*-hIP or, as control, with *anti*-hIP antibody preincubated with the antigenic peptide, corresponding to IC_2 of the hIP, prior to detection with AlexaFluor488 goat *anti*-rabbit secondary antibody. Images were captured at 63x magnification using a Zeiss microscope and Axiovision software.